



# Differentiated Human SH-SY5Y Cells Provide a Reductionist Model of Herpes Simplex Virus 1 Neurotropism

✉ Mackenzie M. Shipley, Colleen A. Mangold, Chad V. Kuny, ✉ Moriah L. Szpara

Department of Biochemistry and Molecular Biology and Huck Institutes of the Life Sciences, Pennsylvania State University, University Park, Pennsylvania, USA

**ABSTRACT** Neuron-virus interactions that occur during herpes simplex virus (HSV) infection are not fully understood. Neurons are the site of lifelong latency and are a crucial target for long-term suppressive therapy or viral clearance. A reproducible neuronal model of human origin would facilitate studies of HSV and other neurotropic viruses. Current neuronal models in the herpesvirus field vary widely and have caveats, including incomplete differentiation, nonhuman origins, or the use of dividing cells that have neuropotential but lack neuronal morphology. In this study, we used a robust approach to differentiate human SH-SY5Y neuroblastoma cells over 2.5 weeks, producing a uniform population of mature human neuronal cells. We demonstrate that terminally differentiated SH-SY5Y cells have neuronal morphology and express proteins with subcellular localization indicative of mature neurons. These neuronal cells are able to support a productive HSV-1 infection, with kinetics and overall titers similar to those seen in undifferentiated SH-SY5Y cells and the related SK-N-SH cell line. However, terminally differentiated, neuronal SH-SY5Y cells release significantly less extracellular HSV-1 by 24 h postinfection (hpi), suggesting a unique neuronal response to viral infection. With this model, we are able to distinguish differences in neuronal spread between two strains of HSV-1. We also show expression of the antiviral protein cyclic GMP-AMP synthase (cGAS) in neuronal SH-SY5Y cells, which is the first demonstration of the presence of this protein in non-epithelial cells. These data provide a model for studying neuron-virus interactions at the single-cell level as well as via bulk biochemistry and will be advantageous for the study of neurotropic viruses *in vitro*.

**IMPORTANCE** Herpes simplex virus (HSV) affects millions of people worldwide, causing painful oral and genital lesions, in addition to a multitude of more severe symptoms such as eye disease, neonatal infection, and, in rare cases, encephalitis. Presently, there is no cure available to treat those infected or prevent future transmission. Due to the ability of HSV to cause a persistent, lifelong infection in the peripheral nervous system, the virus remains within the host for life. To better understand the basis of virus-neuron interactions that allow HSV to persist within the host peripheral nervous system, improved neuronal models are required. Here we describe a cost-effective and scalable human neuronal model system that can be used to study many neurotropic viruses, such as HSV, Zika virus, dengue virus, and rabies virus.

**KEYWORDS** neuron, virus, HSV-1, differentiation, infection, SH-SY5Y, SK-N-SH, cGAS, herpes simplex virus

Herpes simplex virus 1 (HSV-1) is a double-stranded DNA virus in the *Alphaherpesvirinae* subfamily of *Herpesviridae*. The virus establishes primary infection in humans through entry at skin and mucosal sites. The orofacial region is the most common site of initial infection, but genital tract infections are also prevalent (1). It is estimated

Received 8 June 2017 Accepted 19 September 2017

Accepted manuscript posted online 27 September 2017

**Citation** Shipley MM, Mangold CA, Kuny CV, Szpara ML. 2017. Differentiated human SH-SY5Y cells provide a reductionist model of herpes simplex virus 1 neurotropism. *J Virol* 91:e00958-17. <https://doi.org/10.1128/JVI.00958-17>.

**Editor** Rozanne M. Sandri-Goldin, University of California, Irvine

**Copyright** © 2017 American Society for Microbiology. All Rights Reserved.

Address correspondence to Moriah L. Szpara, [moriah@psu.edu](mailto:moriah@psu.edu).

that approximately 67% of the world's population is infected orally with HSV-1, while approximately 19% are infected genitally with either HSV-1 or -2 (2, 3). In addition to replicating at the peripheral epithelium, HSV is able to establish latent infections in sensory and autonomic ganglia via retrograde axonal transport into the peripheral nervous system. Once latent, the virus can reactivate at any time in response to stimuli such as physical or emotional stress or compromised immunity. Cell- or tissue-specific factors play a role in the establishment of a lytic versus latent infection, as evidenced by the ability of the virus to induce latency in neurons, while infection in nonneuronal cells remains productive (1). However, viral replication does occur in human neurons. Evidence suggests that neurons can undergo productive infection prior to establishing a quiescent, latent state, and neurons also actively produce virus during reactivation from latency (4, 5). At present, there is no vaccine available to prevent HSV infection. Current antiviral therapies treat the active, replicating stage of the virus, leaving the latent phase unaffected. Development of new antivirals that target latent virus in neurons will be key to ending lifelong infections. A reproducible *in vitro* model of mature, homogeneous, human neurons will facilitate the search for new antivirals that target HSV latency and reactivation (6).

Immune molecules play a key role during HSV-1 infection in both the epithelium and the peripheral nervous system. The severity of HSV-1 disease that an individual experiences is thought to depend on a combination of viral virulence factors, local environmental stimuli (such as UV exposure), and the ability of the host's immune system to combat the virus (7–11). Pathogen recognition to initiate the host immune response occurs via many different pathways and mechanisms (12–14). Cyclic GMP-AMP synthase (cGAS) and interferon gamma (IFN- $\gamma$ )-inducible protein 16 (IFI16) are two viral DNA sensors shown to be important for detecting HSV-1 in epithelial cells and eliciting a downstream immune response through interferon regulatory factor 3 (IRF-3) (15–21). Recent work with epithelial cells suggests that IFI16 is required for direct detection of and binding to HSV-1 DNA in the nucleus, while cGAS acts to stabilize this interaction (20). However, it is unknown whether this same mechanism exists in neurons. It is known that neurons express Toll-like receptor 3 (TLR-3) in both the brain and peripheral nerves *in vivo* (22–24). It has also been shown that TLR-3 can play diverse antiviral roles in the host and that its function may be dependent upon other immune factors and/or the specificity of the invading pathogen (25, 26). Neurons express major histocompatibility complex (MHC) class I molecules *in vivo* (27, 28), and expression of these molecules is increased after infection with murine hepatitis virus or HSV (29, 30). Since neurons *in vivo* express DNA sensors that serve as detectors of viral infection, it is important to determine if *in vitro* neuronal models reflect this capability as well.

Current *in vitro* research on HSV-1 infection of neurons is often performed using murine neurons, totipotent stem cells, or undifferentiated neuroblastoma cells (31–34). Although useful, these systems have caveats, such as incomplete neuronal differentiation, ongoing cell division, variability in neuronal phenotypes, nonhuman origins, and/or unstable karyotypes (31, 35, 36). These have negative impacts on experimental reproducibility. Furthermore, the use of rodent instead of human neurons introduces additional caveats, such as differences in the outcome of transcription factor cascades in mice versus humans (37–39). Herpesviruses are also highly host specific, having coevolved with their hosts over millions of years (40). HSV-1 penetration into the central nervous system (CNS) is uncommon in human adults, as is severe neurologic disease such as encephalitis (41, 42). Murine model systems reach this encephalitic outcome more readily than human HSV-1 infections (8, 43, 44). These findings highlight the importance of using a system that reflects the attributes of human neurons, and the need to corroborate prior results from murine models in a human neuronal environment.

Prior data have established the ability of the chromosomally stable human SH-SY5Y neuroblastoma cell line to be differentiated into mature neuronal cells (45–48). SH-SY5Y neuroblastoma cells are a subclone derived from the parent cell line SK-N-SH (47). Undifferentiated, dividing SH-SY5Y cells become terminally differentiated over the

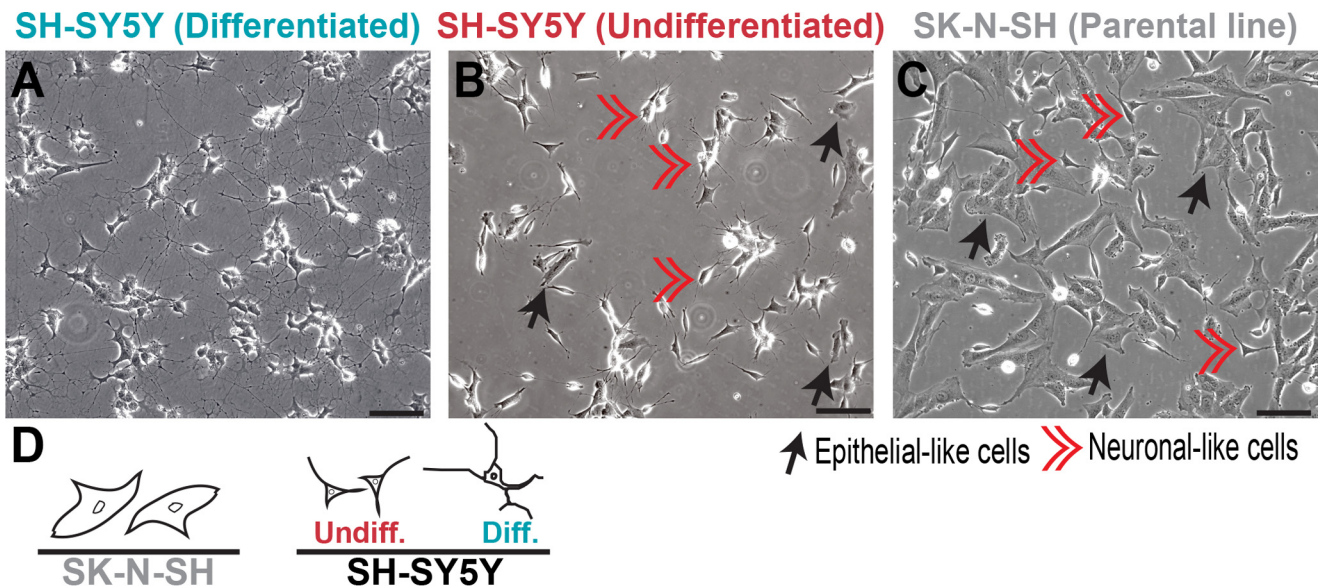


**FIG 1** Terminally differentiated neuronal SH-SY5Y cells are morphologically distinct from undifferentiated SH-SY5Y cells and SK-N-SH cells. (A) Terminally differentiated SH-SY5Y cells appear neuronal after 2.5 weeks of differentiation. At 2 days postplating, mixed cell morphologies are visible in undifferentiated SH-SY5Y cells (B) and in the parent cell line SK-N-SH (C). Black arrows indicate epithelial-like cells, and red arrowheads indicate neuronal-like cells. (D) Traced outlines of representative cells, approximately 1.5 times their actual size. Scale bars represent 100  $\mu\text{m}$ .

course of 2.5 weeks. Terminally differentiated in this case is defined as a state in which the cells are no longer dividing, are neurotrophin dependent, and are committed to a neuronal phenotype. During this transition, epithelial-like cells are removed through a combination of serum starvation and the addition of retinoic acid (RA). Serum starvation has been shown to induce apoptosis in epithelial cells (49, 50), while RA activates tyrosine receptor kinase B (Trk) in neuronal cells, leading to survival of only the neurotrophin-dependent cells (45, 51, 52). As neurotrophic factors are added and the cultures are replated onto extracellular matrix (ECM), the cells begin to grow and develop neuritic processes, ultimately forming an extensive meshwork of neurites (53). Eventually, there are few to no epithelial cells remaining, resulting in a homogeneous population of cells that resemble mature human neurons.

Here we characterize the use of terminally differentiated SH-SY5Y neuronal cells (53) as a model for studying HSV-1–neuron interactions during the course of infection. This system provides a model with a natural host-virus species pairing which is amenable to both single-cell imaging and bulk biochemical approaches. We demonstrate that terminally differentiated SH-SY5Y cells express neuronal proteins with a localization that is indicative of mature neurons. We show that in a single round of replication, HSV-1 strain McKrae reaches overall titers in terminally differentiated SH-SY5Y neuronal cells similar to those in the mixed population of parental SK-N-SH cells and the undifferentiated SH-SY5Y cell line. However, the neuronal SH-SY5Y cells release significantly less extracellular virus by 24 h postinfection (hpi). In an assay focused on cell-to-cell spread in SH-SY5Y neuronal cells, we were able to detect differences in neuronal spread between the HSV-1 strains McKrae and KOS. These data suggest that this neuronal model may provide an opportunity to quantify the phenotypes of neurotropic viruses *in vitro*. We demonstrate for the first time that these neuronal cells express the host antiviral factor cGAS, which is known to elicit a downstream innate immune response through the detection of viral pathogens.

## RESULTS

### Terminally differentiated SH-SY5Y cells exhibit mature neuronal morphology.

All three cell populations examined in this study (Fig. 1) have been used previously to study neuronal aspects of host-virus interactions (Table 1). However, SK-N-SH cells and

**TABLE 1** Use of undifferentiated SH-SY5Y and SK-N-SH cells, in contrast to terminally differentiated SH-SY5Y neuronal cells, in studies of neurotropic viruses

Virus type	Virus(es) studied using the indicated cell type (reference[s])		
	SK-N-SH cell line	Undifferentiated SH-SY5Y cells	Differentiated SH-SY5Y cells <sup>a</sup>
DNA viruses	HSV-1 (103, 106–116), <sup>b</sup> JC virus (117)	Adenovirus (118), Epstein-Barr virus (119), HSV-1 (106, 120–125), Kaposi's sarcoma herpesvirus (119), JC virus (117), mouse gammaherpesvirus 68 (126)	Bovine herpesvirus (127), HSV-1 (45, 48, 121), varicella-zoster virus (46, 128)
RNA viruses	Borna disease virus (129), dengue virus (130), enterovirus 71 (131), Japanese encephalitis virus (132, 133), measles virus (134–136), Menangle virus (153), rabies virus (111, 154, 155), Sindbis virus (156), tick-borne encephalitis virus (157), Tioman virus (153), Tofla virus (137)	Dengue virus (138), enterovirus 71 (139, 140), HIV (141, 142), human endogenous retrovirus (143), Japanese encephalitis virus (144, 145), mumps virus (158)  Newcastle disease virus (159), poliovirus (55), porcine reproductive and respiratory syndrome virus (160), Puumala virus (161), rabies virus (154), West Nile virus (54), western equine encephalitis virus (56), vesicular stomatitis virus (162), Zika virus (146)	Chikungunya virus (147), enterovirus 71 (148), HIV (149–152), human T-cell lymphotropic virus (163)

<sup>a</sup>Includes both short (5 to 7 days) and long differentiation (>10 days) protocols.

<sup>b</sup>In the studies described in references 115 and 116, SK-N-SH cells were differentiated with retinoic acid for 7 days.

undifferentiated SH-SY5Y cells experience ongoing cell division and contain mixed populations of epithelial-like and neuronal-like cells (47). This raised the possibility that using these cells in an undifferentiated state would reflect epithelial or mixed cell population responses to infection, rather than the intended focus on neuronal responses. Terminally differentiated SH-SY5Y cells provide a homogeneous population of human neuronal cells that can be used to study neuron-virus interactions for a variety of neurotropic viruses that impact public health (54–57). We investigated whether differentiated SH-SY5Y neuronal cells served as a suitable platform to study human host-virus interactions in a species-matched manner.

Differentiation of SH-SY5Y cells for 2.5 weeks, with removal of serum and addition of neurotrophic factors, yielded neuronal cells (see Materials and Methods for details). Morphologically, these differentiated neuronal cells were distinct from both the parental SK-N-SH cell line and from the undifferentiated SH-SY5Y progenitor cells (Fig. 1). Terminally differentiated neuronal cells had a smaller soma with extensive neurite projections (Fig. 1A), whereas the parental SK-N-SH cells had an epithelial appearance with a larger soma (Fig. 1C). Undifferentiated SH-SY5Y cells were a heterogeneous population of epithelial-like cells that resembled those of the SK-N-SH parent line, and neuronal-like cells with short neurites (Fig. 1B).

Previously published data have demonstrated that differentiated human neurons have enhanced expression of specific neuronal proteins compared to that of nonneuronal cells, including neurofilament components, synaptic vesicle proteins, and growth-associated proteins, such as growth-associated protein 43 (GAP-43) (45, 46, 58, 59). We used immunofluorescence (IF) to ascertain whether terminally differentiated SH-SY5Y cells express localized neuronal markers similar to those found in mature neurons. Following 2.5 weeks of differentiation, both the undifferentiated (Fig. 2A) and differentiated (Fig. 2B) SH-SY5Y cells expressed microtubule-associated protein 2 (MAP-2), with more extensive localized staining visible in the differentiated cells due to their expansive neurite network. Both undifferentiated and differentiated SH-SY5Y cells expressed the unphosphorylated form of neurofilament heavy chain (NF-H) protein, which localized in the perinuclear space (Fig. 2A and B). Phosphorylated NF-H (p-NF-H) is a marker of axons in mature neurons (60). We found that this protein was expressed only in the differentiated SH-SY5Y cells, where it localized in axonal projections (Fig. 2C and D). Synaptic vesicle protein 2 (SV2) specifically localizes at synapses in neurons (61), and only the neuronal SH-SY5Y cells appeared to have concentrated puncta of SV2 present in their dense network of neurites (Fig. 2E to H). Based on morphology and immunofluorescence data, terminally differentiated SH-SY5Y cells appeared neuronal and fully polarized.

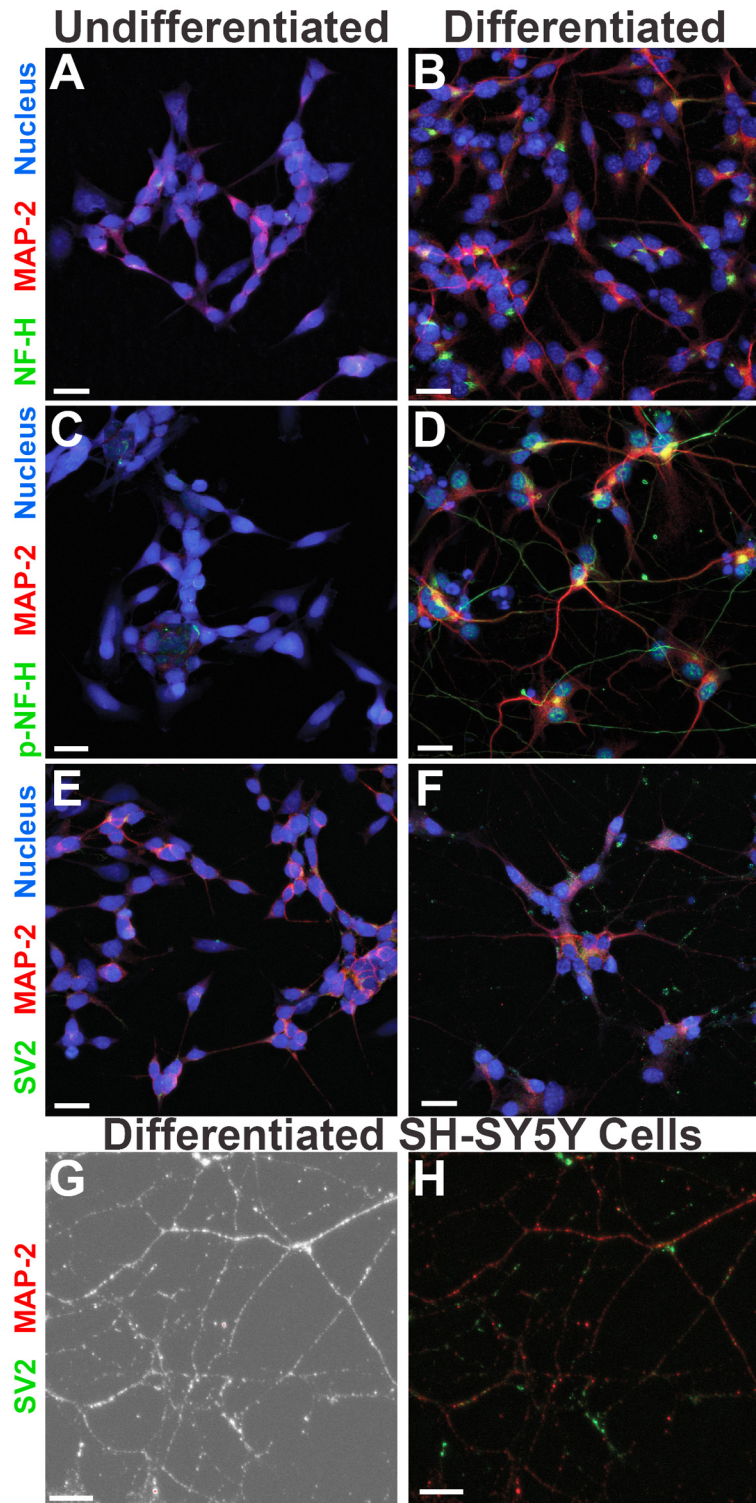


**FIG 2** Terminally differentiated SH-SY5Y neuronal cells show distinct localization of cytoskeletal and synaptic markers. Differentiation of SH-SY5Y cells for 2.5 weeks yields morphologically distinct localization of neuronal proteins (B, D, and F), in contrast to that seen in undifferentiated SH-SY5Y cells (A, C, and E). Higher magnification of differentiated SH-SY5Y neurites shown in phase-contrast (G) reveals further details of microtubule and synaptic vesicle staining (H). The 2.5-week differentiation process includes the addition of RA, neurotrophic factors, and ECM proteins. MAP-2, microtubule associated protein 2; NF-H, unphosphorylated neurofilament heavy chain; p-NF-H, phosphorylated neurofilament heavy chain; SV2, synaptic vesicle protein 2; Nucleus, nuclear/DNA stain. Images were taken with an Olympus FV10i confocal microscope at a magnification of  $\times 60$ , and the scale bars represent  $20 \mu\text{m}$ . Images in panels G and H were taken with an additional  $2.6\times$  digital zoom, and the scale bars represent  $10 \mu\text{m}$ .

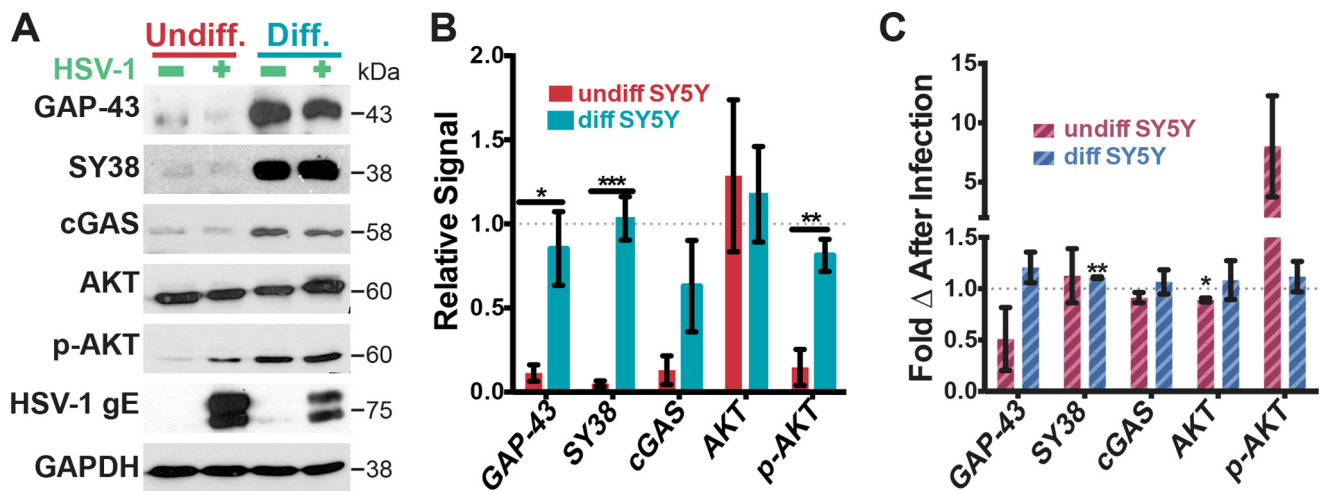


**FIG 3** Neuronal differentiation significantly impacts expression of GAP-43, SY38, and p-AKT. (A) Proteins involved in neuronal differentiation, growth, and signaling are expressed at high levels in terminally differentiated SH-SY5Y neuronal cells. The neuronal growth-associated protein GAP-43 and synaptic vesicle marker SY38 are expressed at significantly higher levels in differentiated SH-SY5Y neuronal cells than in the undifferentiated progenitor cells. The cytoplasmic DNA sensor cGAS, as part of the intrinsic immune response, is expressed in both the undifferentiated and neuronal SH-SY5Y cells. While AKT levels appear equal in undifferentiated and neuronal SH-SY5Y cells, p-AKT levels are significantly higher in differentiated neuronal cells. HSV-1 glycoprotein E (gE) serves as a positive control for viral infection. GAPDH serves as a loading control. Images are representative of three biological replicates. Twenty micrograms of protein was loaded for each cell population. (B) Quantification of the effects of differentiation on protein expression levels in uninfected SH-SY5Y cells that are either undifferentiated (red) or neuronally differentiated (blue). The signal of each protein target was normalized and expressed relative to GAPDH loading levels. p-AKT signal was normalized to AKT. Multiple *t* tests were performed with alpha at 5.0%. \*,  $P = 0.03$ ; \*\*,  $P = 0.01$ ; \*\*\*,  $P = 0.002$ . (C) HSV-1 infection has a significant impact on SY38 and AKT protein levels in SH-SY5Y cells. With the exception of p-AKT induction in undifferentiated SH-SY5Y cells and SY38 expression in differentiated SH-SY5Y neuronal cells, most protein levels are unchanged following HSV-1 infection. Results are presented as fold change of expression following infection. One-sample *t* tests were performed on each protein target against a hypothetical uninfected value of 1. \*,  $P = 0.03$ ; \*\*,  $P = 0.007$ . See the text for protein descriptions and Materials and Methods for antibody details.

### Neuronal differentiation significantly impacts expression of GAP-43, SY38, and phospho-AKT (p-AKT).

After we determined that the differentiated SH-SY5Y cells had specific localization and expression of neuronal markers, we next investigated protein levels by Western blotting (WB). We compared protein levels in the undifferentiated and terminally differentiated neuronal states, as well as in the presence of HSV-1 infection. We examined total cell lysates from uninfected cells versus those from cells infected at a multiplicity of infection (MOI) of 10 with HSV-1 McKrae and harvested at 6 hpi. We found that differentiated SH-SY5Y cells had high expression levels of the neuronal proteins GAP-43 and synaptic vesicle protein 38 (SY38) (Fig. 3A and B), corroborating the IF data. GAP-43 phosphoprotein is expressed in neuronal growth cones and aids in the extension and outgrowth of neurites in developing neurons (62). We found that GAP-43 expression was significantly higher in the differentiated SH-SY5Y neuronal cells than in the undifferentiated SH-SY5Y cells. However, no significant changes in the expression of this neuronal protein occurred following HSV-1 infection (Fig. 3C). Synaptic vesicle protein 38, also known as synaptophysin, is an integral membrane glycoprotein expressed in presynaptic vesicles of neurons (63). Synaptophysin was expressed at significantly higher levels in the differentiated SH-SY5Y neuronal cells than in undifferentiated SH-SY5Y cells (Fig. 3A and B). SY38 expression in differentiated SH-SY5Y neuronal cells also appeared to significantly increase during HSV-1 infection (Fig. 3C). Taken together, these data demonstrated that terminally differentiated SH-SY5Y cells have high expression of neuronal proteins and that undifferentiated SH-SY5Y cells do not reflect this aspect of neurobiology.

To investigate the response of these neuronal cells to HSV-1 infection, we measured the levels of several antiviral and stress-associated proteins before and after infection. Based on prior data (20, 65), we hypothesized that viral infection would induce a stress response within cells, and that this might alter the expression profile of these proteins following infection. We found that protein kinase B (AKT) expression levels remained similar between differentiation states and that viral infection appeared to significantly

affect AKT expression only in undifferentiated SH-SY5Y cells (Fig. 3). Phosphorylation and activation of AKT (to form phospho-AKT) occurred in both cell types during infection. However, when the cells were not infected, phospho-Akt (p-AKT) was apparent only in terminally differentiated SH-SY5Y neuronal cells (Fig. 3). We also examined the expression levels of the antiviral protein cGAS, which has been implicated in detecting and binding to HSV-1 viral DNA and eliciting a downstream immune response (20). This antiviral protein is also involved in sensing many other viral pathogens (66). We found that cGAS expression levels were higher in the differentiated SH-SY5Y neuronal cells than in the undifferentiated progenitor cells. cGAS expression did not appear to be affected by HSV-1 at 6 hpi (Fig. 3).

**Neuronal SH-SY5Y cells release less extracellular virus during lytic HSV-1 infection.** Next, we wanted to determine whether a commonly used strain of HSV-1 replicated differently in the neuronal cells than in the progenitor cells during a single round of replication. Using the HSV-1 strain McKrae (67–70), we measured the progression of productive HSV-1 infection in this neuronal model compared to the epithelial progenitor cells included in Fig. 1. We performed high-MOI (single-step) growth curves in parental SK-N-SH cells, undifferentiated SH-SY5Y cells, and terminally differentiated SH-SY5Y neuronal cells. Each cell type was infected with HSV-1 McKrae at an MOI of 10, and we collected cell-associated virus and released-virus (cell-free) samples at 1, 6, 8, 12, 18, and 24 hpi. Quantification of virus production suggested that all three cell types had similar viral kinetics and overall titers during a single round of replication (Fig. 4A). However, virion production in SK-N-SH cells appeared to peak earlier (Fig. 4A, 1 to 6 hpi). In addition, terminally differentiated SH-SY5Y neuronal cells released significantly less extracellular virus than the mixed cell populations by 24 hpi (Fig. 4A). These data demonstrated that neuronal SH-SY5Y cells were fully replication competent for HSV-1 and suggested the potential for neuronal phenotypes distinct from those observed in epithelial-like cells.

Phase-contrast images of all three cell types infected at an MOI of 10 with HSV-1 McKrae demonstrated cytopathic effects (CPE) over time (Fig. 4B; see also Movie S1 in the supplemental material). Morphological changes in the neuronal cells were identified as early as 6 hpi, including retraction of neurites and loss of substrate attachment. Alterations in the epithelial progenitor cells were not visible until approximately 12 hpi. To investigate whether these cells undergo cell death via caspase-mediated apoptosis, inactive procaspase 3 cleavage was assessed at 2, 4, 6, 12, and 24 hpi (Fig. 4C). Decreased procaspase 3 expression was evident by 6 hpi in the neuronal cells, while procaspase 3 levels did not appear to decrease by 24 h in the undifferentiated SH-SY5Y cells or SK-N-SH progenitor cells. These data suggested that caspase 3 was active early in viral infection of the neuronal cells. These data further supported the morphological changes observed following viral infection over time in the differentiated SH-SY5Y neuronal cells.

**Neuronal SH-SY5Y cells reveal distinct phenotypes of cell-to-cell spread for different strains of HSV-1.** We next determined whether we could distinguish between two frequently studied strains of HSV-1 based upon their ability to replicate and spread from cell to cell in this *in vitro* neuronal model. For this low-MOI (0.01) experiment, we infected differentiated SH-SY5Y neuronal cells with either HSV-1 McKrae or HSV-1 KOS in the presence of 0.1% pooled human serum (see Movie S2). The yield of HSV-1 McKrae infection was approximately 1 log higher than for HSV-1 KOS at 72 hpi (Fig. 5A). Morphologically, the differentiated SH-SY5Y neuronal cells appear to undergo CPE-induced cell death at similar rates over the course of 72 h with both virus strains (Movie S2). In contrast, performing this experiment with both undifferentiated SH-SY5Y cells and Vero cells revealed no difference in the rate of replication between HSV-1 McKrae and HSV-1 KOS (Fig. 5B). It is notable that Vero cells, a monkey kidney cell line often used to prepare viral stocks of HSV-1, produce a viral titer almost a log higher than undifferentiated SH-SY5Y cells (Fig. 5B). We also compared HSV-1 strains McKrae and KOS in a high-MOI infection of neuronal cells and Vero cells and found no difference in the replication rates over this single round of replication (data not shown). These data

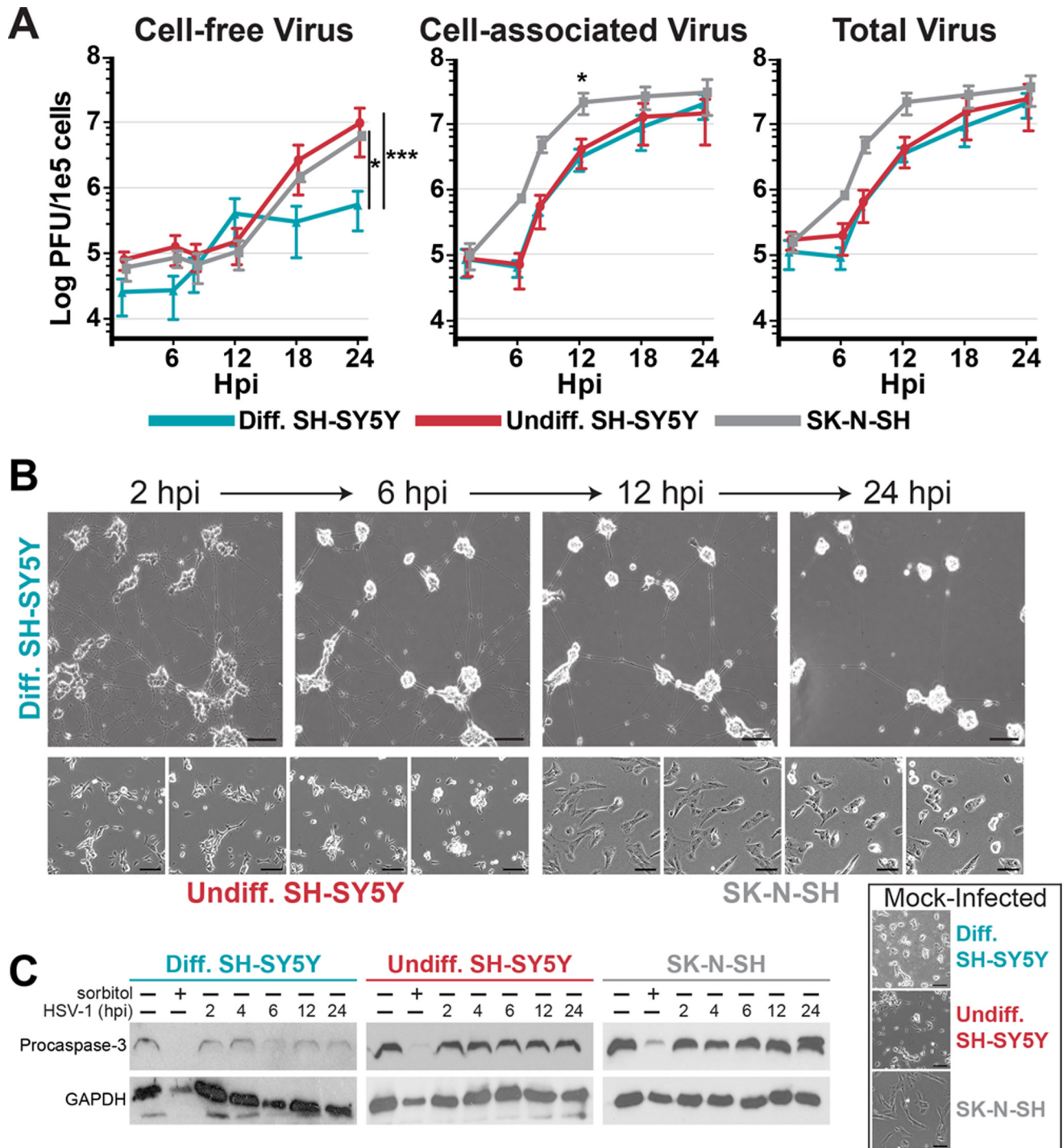


**FIG 4** Neuronal SH-SY5Y cells release less extracellular virus during lytic HSV-1 infection. (A) Single-step growth curves of viral replication kinetics in differentiated SH-SY5Y neuronal cells (blue), undifferentiated SH-SY5Y cells (red), and SK-N-SH cells (gray). Each cell type was infected with HSV-1 McKrae at an MOI of 10. Titers are plotted as log PFU per 100,000 cells. Cell-free viral titers, cell-associated viral titers, and combined total viral titers include three biological replicates. A 2-way analysis of variance (ANOVA) was performed for each graph: for cell-free virus, \*,  $P = 0.0229$ ; \*\*\*,  $P = 0.004$ ; for cell-associated virus, \*,  $P = 0.0452$ . Each graph displays the average from the three replicates, and the error bars represent the standard errors of the means (SEM). (B) Time-lapse images reveal morphological changes in differentiated SH-SY5Y neuronal cells, undifferentiated SH-SY5Y cells, and SK-N-SH cells during infection with HSV-1 McKrae at a high MOI (10). Initial changes in neuronal cell morphology begin at 6 hpi, with clear neurite retraction by 12 hpi. At 24 hpi, neuronal morphology is markedly different and few neurites remain. Following viral infection in the undifferentiated SH-SY5Y cells and SK-N-SH cells, morphological changes are not visible until 12 hpi. By 24 hpi, the undifferentiated SH-SY5Y cells appear to all be infected and rounded up. The SK-N-SH cells appear to be more robust, with only about 50% of cells rounded up by 24 hpi. The scale bar represents 25  $\mu$ m. Images are representative of those from three biological replicates. (C) Procaspase 3 expression data demonstrate cleavage and activation of caspase 3 in differentiated SH-SY5Y neuronal cells, undifferentiated SH-SY5Y cells, and SK-N-SH cells over a time course of 24 hpi with HSV-1 McKrae (MOI of 10). Sorbitol-induced osmotic shock serves as a positive control for activation of caspase 3. Blots are representative of those from two biological replicates.



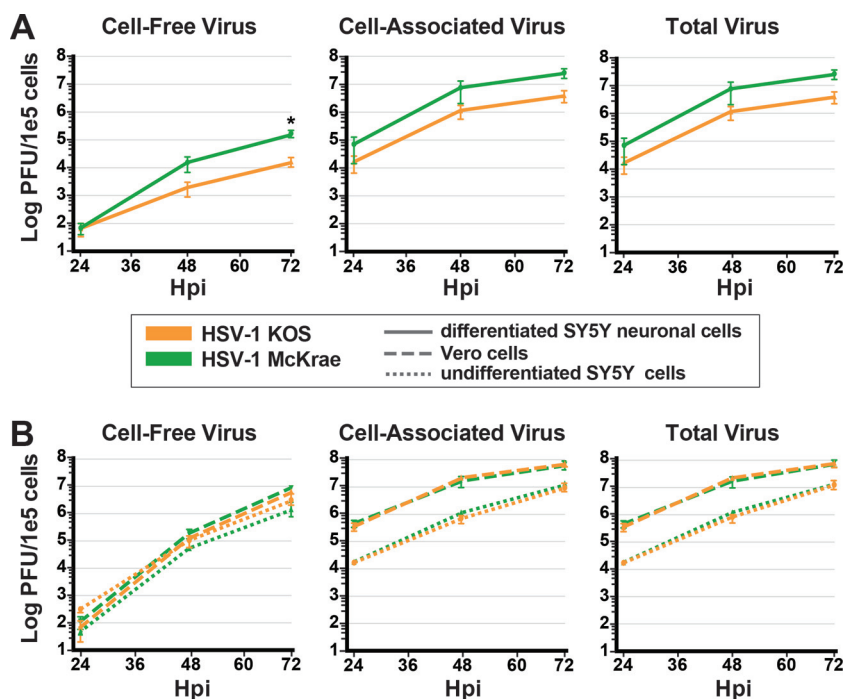


**FIG 5** Neuronal SH-SY5Y cells reveal distinct phenotypes of cell-to-cell spread for different strains of HSV-1. Following a low-MOI infection with sample collection at 24, 48, and 72 hpi, neuronal SH-SY5Y cells (A) but not undifferentiated SH-SY5Y cells or Vero cells (B) distinguish between two phenotypically distinct viral strains. For these multistep growth curves, all three cell types were infected with HSV-1 McKrae (green) or HSV-1 KOS (orange) at an MOI of 0.01 in the presence of 0.1% pooled human serum. Data include three biological replicates, and error bars represent the SEM. Multiple *t* tests were performed for neuronal SH-SY5Y cells, with alpha of 5.0%. \*, *P* = 0.04.

suggested that cell-to-cell-spread assays, such as this low-MOI (multistep) growth curve in differentiated SH-SY5Y neuronal cells, may prove useful in screening HSV-1 strains for potential differences in their abilities to replicate and spread in a neuron-specific manner.

**Differentiated neuronal cells have a unique pattern of cGAS expression compared to MRC5 cells before and during HSV-1 infection.** Prior research has shown that IFI16 and cGAS can act together to detect HSV-1 viral DNA in the nuclei of epithelial cells following HSV-1 infection (19, 20). However, the expression of these factors in human neurons has not yet been investigated. Through confocal microscopy, we found that differentiated SH-SY5Y neuronal cells expressed cGAS both before and during HSV-1 infection (Fig. 6A). Expression of IFI16 was not sufficiently above the level of neuronal autofluorescence for a robust comparison, and was therefore excluded from further analysis (data not shown). cGAS localized to the cytoplasm of uninfected differentiated SH-SY5Y neuronal cells, which was consistent with prior observations in epithelial cells. No significant change in cGAS expression levels (Fig. 3A) or localization (Fig. 6A) occurred following infection with HSV-1 McKrae at 3 or 6 hpi. These neuronal localization data were different from what has been reported for cGAS expression in epithelial cell types. To confirm the efficacy of the cGAS and IFI16 detection used in this study, we examined both proteins in human lung fibroblasts (MRC5) (Fig. 6B). MRC5 fibroblasts expressed IFI16 in the nucleus and cGAS in the cytoplasm prior to HSV-1 infection. Following viral infection, we observed both IFI16 and cGAS in the nuclei of these epithelial cells, as has been shown in other epithelial cell types. Taken together, these data suggested that terminally differentiated SH-SY5Y cells provide a homogeneous and reproducible model system for the investigation of HSV-1 infection and cGAS antiviral signaling from a neuronal perspective *in vitro*.

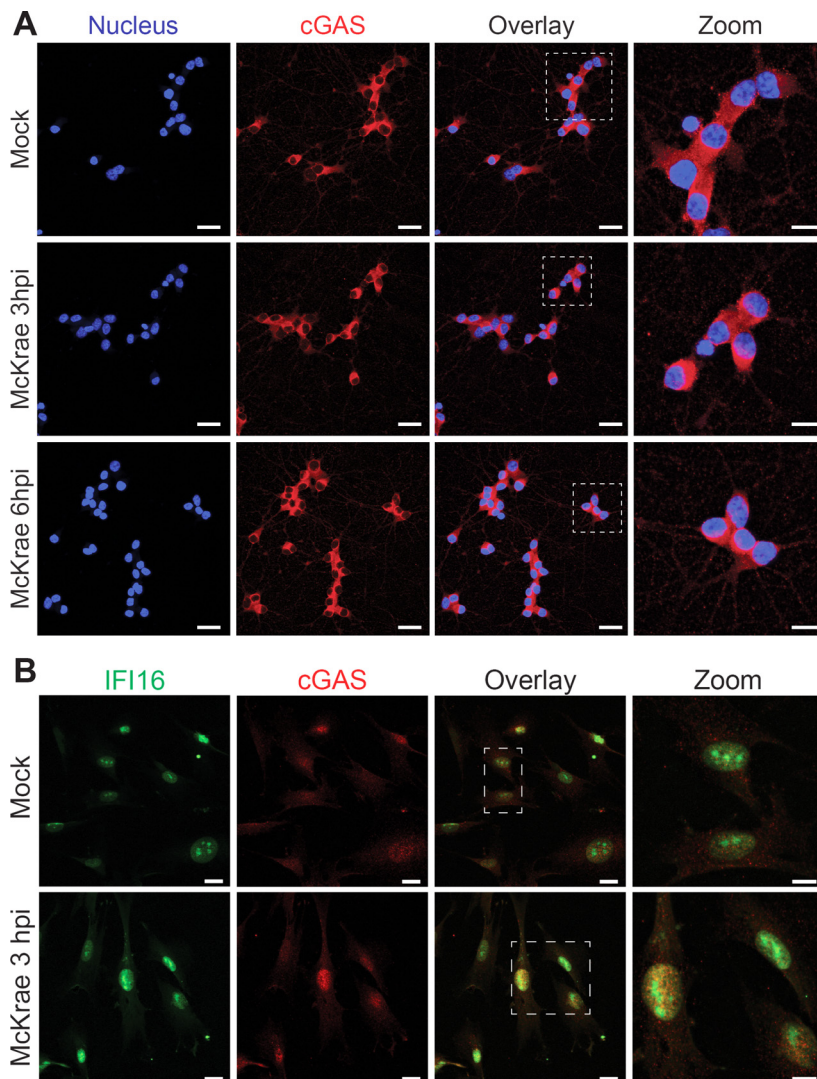


**FIG 6** Differentiated neuronal cells have a unique pattern of cGAS expression compared to MRC5 cells before and during HSV-1 infection. Differentiated neuronal cells express the antiviral protein cGAS in the cytoplasm and in neurites both before and after HSV-1 infection, while MRC5 cells express cGAS and IFI16 in the nucleus following HSV-1 infection. (A) Terminally differentiated SH-SY5Y neuronal cells were infected at an MOI of 10 with HSV-1 McKrae and then fixed and processed for cGAS expression at 3 hpi or 6 hpi. Scale bars represent 20  $\mu\text{m}$ . The zoomed-in images were acquired with a 168 $\times$  objective, and scale bars represent 10  $\mu\text{m}$ . (B) MRC5 fetal lung fibroblasts were infected at an MOI of 10 with HSV-1 McKrae and then fixed and processed for immunofluorescence at 3 hpi. Scale bars represent 20  $\mu\text{m}$ . The zoomed-in images were acquired with a 156 $\times$  objective, and scale bars represent 10  $\mu\text{m}$ . Images were taken with an Olympus FV10i confocal microscope with a 60 $\times$  objective.

## DISCUSSION

Here we describe an *in vitro* model of differentiated human neuronal cells that serves as a facile system for biochemical and molecular dissection of HSV-1-neuron interactions. We characterized the neuronal phenotype of terminally differentiated SH-SY5Y cells and compared these data to those for undifferentiated SH-SY5Y progenitor cells and the parental SK-N-SH cell line. We showed that terminally differentiated SH-SY5Y cells possessed neuronal morphology that was distinct from that of undifferentiated SH-SY5Y cells or SK-N-SH cells. Specifically, we demonstrated that terminally differentiated SH-SY5Y cells expressed proteins associated with a mature neuronal phenotype, including the appropriate localization of markers for axons, dendrites, and synapses. This model yields homogeneous populations of human neuronal cells, which

provide a species-matched platform with which to explore the molecular and cellular mechanisms of viral infection in humans.

Consistent with published data (45, 46), we found that terminally differentiated SH-SY5Y cells expressed neuronal proteins and appeared to have both axons (via p-NF-H) and dendrites (via MAP-2). MAP-2 associates with tubulin to help promote the assembly of microtubules in both axons and dendrites of neurons (45). *In vivo*, the axonal localization of p-NF-H occurs only after the neurofilaments have entered into mature axons (60); likewise, p-NF-H is only observed in the terminally differentiated SH-SY5Y neuronal cells and not in undifferentiated SH-SY5Y precursor cells. Differentiated SH-SY5Y neuronal cells appeared to have synapses, based on the expression and localization of SV2 and the high total protein levels of synaptophysin (SY38) (Fig. 2 and 3) (61, 63).

Herpesvirus infection triggers activation of stress response genes and pathogen recognition receptors (19, 20, 71). Protein kinase B, also known as AKT, is a serine/threonine kinase that is part of the phosphatidylinositol 3-kinase (PI3-K) pathway (72, 73). Both AKT and PI3-K signaling are required for RA-induced differentiation of neuroblastoma cells (74). Neuronal SH-SY5Y cells had significantly higher expression levels of p-AKT than undifferentiated SH-SY5Y cells (Fig. 3). Since AKT is known to undergo autophosphorylation and activation (p-AKT) in response to stimulation of Trk from neurotrophin binding (52, 72, 73), the increased level of p-AKT in neuronal SH-SY5Y cells (Fig. 3) likely reflects neuronal differentiation and Trk activation (75). Increased p-AKT levels following viral infection (Fig. 3) match prior findings by other groups (76–78). Activated p-AKT functions in apoptosis, protein synthesis, and cell growth (79–81), and viruses, including HSV-1, have been shown to hijack this pathway during infection (76–78, 82, 83). Prior data have shown that continuous signaling via the PI3-K pathway and p-AKT in superior cervical ganglion-derived neurons is also critical for the maintenance of HSV-1 latency *in vitro* (65, 84, 85). This provides an exciting avenue for further study, as a neuronal system primed with high levels of p-AKT may facilitate development of an improved model for HSV-1 latency.

We also found that neuronal SH-SY5Y cells expressed the antiviral sensor cGAS (Fig. 3A and Fig. 6A). This protein elicits activation of interferon regulatory factor 3 (IRF-3) via the stimulator of interferon gene (STING)-dependent pathway, resulting in activation of the type I interferon (IFN) pathway and production of IFN- $\beta$  (16, 86). cGAS has been shown to detect many viral pathogens in the cytosol (66) and is therefore an important component of the host antiviral defense system. Additionally, cGAS is known to interact with activated p-AKT, which phosphorylates cGAS and inhibits activation of the downstream interferon pathway (87). It is hypothesized that in epithelial cells, IFI16 detects and binds directly to HSV-1 DNA in the nucleus (18), with subsequent interaction of cGAS to stabilize IFI16's interaction with the viral DNA (20). We showed for the first time that the antiviral factor cGAS is expressed in human neuronal cells (Fig. 3 and 6A). We also saw that cGAS expression and localization in neuronal cells was different from what has been reported for epithelial cells, such as MRC5 cells (Fig. 6B) (15, 19, 20). cGAS does not appear to translocate to the nucleus of neuronal cells following HSV-1 infection (Fig. 6A). It is possible that the neuroblastoma origin of the SH-SY5Y cells influences their expression and/or localization of cGAS. More work is needed to determine how cGAS is expressed in different types of neurons and how it contributes to the intrinsic and innate responses of the nervous system to infection.

At present, our understanding of viral neuroinvasion is based on mouse models of HSV-1 infection. The herpesvirus field lacks an *in vitro* proxy measurement for neuroinvasion *in vivo*. *In vivo* comparisons are costly in terms of time, labor, and animal use, and thus, these animal models are not universally employed for every comparison of HSV strains. An *in vitro* model that could serve as a preliminary assessment of neuronal spread and potential for neuroinvasion would enable further cross-comparison of viral strains. We found that using differentiated SH-SY5Y neuronal cells and a low-MOI infection, we are able to distinguish between HSV-1 McKrae and HSV-1 KOS. The HSV-1 McKrae strain reached a 10-fold-higher titer in differentiated SH-SY5Y neuronal cells

than the HSV-1 KOS strain (Fig. 5A). Multiple groups have demonstrated that HSV-1 McKrae is a highly neuroinvasive virus, capable of penetrating into the murine central nervous system and inducing subsequent mortality at a high rate (67, 68, 88). In contrast, HSV-1 KOS was found to be less neuroinvasive, and when introduced at the periphery, it did not induce significant mortality (8, 68, 89). This suggests that the reduced cell-to-cell spread of HSV-1 KOS in neuronal cells may contribute to the observed differences in viral strain neuroinvasion. In addition, HSV-1 KOS is known to carry a defective copy of the viral Us9 protein, which contributes to virion transport in axons (90–92). We do not yet know whether these *in vitro* and *in vivo* strain differences are linked, and therefore, this is an exciting area for future investigation. Moreover, the identical multistep growth curves of HSV-1 McKrae and KOS in undifferentiated SH-SY5Y cells and in Vero cells (Fig. 5B) further emphasize that epithelial cell types are not sufficient for detecting differences in neuronal spread *in vitro*.

Within the herpesvirus field, a diverse array of models have been used to study the latent stage of HSV-1 infection (32, 34, 67, 68, 93). While these models have established the foundation of our understanding of latency and reactivation, there are caveats associated with these systems. For example, nonhuman animal models are frequently used to study a species-specific virus that has coevolved with its human host (33, 67, 68, 93). Existing *in vitro* models for the study of HSV-1 latency have yielded promising insights into its molecular mechanisms, but with caveats such as rodent species origins (34, 65, 93–97) and variable differentiation of human neuronal progenitors (31, 98). Terminally differentiated SH-SY5Y cells provide a homogeneous, mature population of human neuronal cells, which may be ideal for adaptation to the *in vitro* latency models currently applied to rodent neurons (34, 65, 94–97). This idea is further supported by the constitutively high p-AKT levels observed in differentiated SH-SY5Y neuronal cells, since p-AKT is known to support HSV-1 latency in other cell types (65, 84, 85).

In conclusion, this model provides a simplified view in which neuronal cells are the focus, which allows for detailed analyses of virus-neuron interactions *in vitro*. Using this system, we have detected that neuronal cells and epithelial progenitor cells mount different responses to HSV-1 infection. These differences include a more limited release of extracellular virus by differentiated SH-SY5Y neuronal cells, as well as their ability to reveal differences between HSV-1 strains in neuronal cell-to-cell spread phenotypes. These findings warrant future studies to explore how these distinct cellular responses relate to the human biology of HSV-1 infection.

## MATERIALS AND METHODS

**Cells and viruses.** Vero African green monkey kidney cells (ATCC; CCL-81), SK-N-SH neuroblastoma cells (ATCC; HB11), and the SK-N-SH subcloned SH-SY5Y cell line (ATCC; CLR-2266) were maintained at 37°C with 5% CO<sub>2</sub>. Vero cells were cultured in Dulbecco's minimal essential medium (DMEM) with 10% fetal bovine serum (FBS), supplemented with penicillin-streptomycin (Pen/Strep; Life Technologies-Gibco) and L-glutamine (Thermo Fischer Scientific-HyClone). SK-N-SH cells were cultured in Eagle's minimal essential medium (EMEM) using 10% heat-inactivated fetal bovine serum (HIFBS), supplemented with Pen/Strep and L-glutamine. Undifferentiated SH-SY5Y and differentiated SH-SY5Y cells were cultured as previously described (53) in a protocol based on those of Christensen et al. (46) and Encinas et al. (45). Briefly, undifferentiated SH-SY5Y cells were plated in EMEM formulated with HIFBS, Pen/Strep, L-glutamine, and 10 μM RA for 7 days, with medium changes every other day. Cells were then transitioned through two additional medium formulations to slowly deplete serum and add in neurotrophic factors, including brain-derived neurotrophic factor (BDNF) (53). The final medium formulation was neurobasal medium (Life Technologies-Gibco) with Glutamax (Life Technologies-Gibco), Pen/Strep, B-27 (Thermo Fischer Scientific), 1 M KCl, dibutyryl cyclic AMP (Sigma), and BDNF (Sigma). The cells were lightly trypsinized and replated onto new 35-mm<sup>2</sup> dishes on days 7 and 10 of the protocol to preferentially select for transfer and survival of the neuron-like cells. Cells were terminally differentiated at 2.5 weeks and ready to use.

HSV-1 strain McKrae was provided by Lynda Morrison (69, 99). KOS<sub>63D</sub> virus was obtained from Richard Dix (8, 100) and is referred to as KOS throughout. HSV-1 strain F-GS2822, a bacterial artificial chromosome (BAC)-derived virus, was provided by Sarah Antinone and Greg Smith (101). This virus is referred to as F<sub>RED</sub> throughout. Viral stocks were grown and titers were determined on Vero cells using DMEM with 2% FBS and antibiotics.

Unless stated otherwise, infections using HSV-1 McKrae, HSV-1 KOS, and HSV-1 F<sub>RED</sub> were performed as follows. Stocks of virus were freeze-thawed three times and sonicated in a cup holder at 80% amplitude for 10 s on/off using a Q500 ultrasonic processor (QSonica). Virus dilutions were made in

cell-appropriate media (listed above) based on average cell counts and the desired MOI. Cells were infected with the selected virus strain and MOI or mock infected using medium specific for each cell type in a total volume of 200  $\mu$ l per 35-mm<sup>2</sup> plate. Following HSV infection or mock infection, plates were incubated at 37°C for 1 h, with rocking every 15 min. Inocula were aspirated and replaced with fresh cell-appropriate media.

**Antibodies.** The antibodies, sources, hosts, assays, dilutions, and protein targets were as follows: glyceraldehyde-3 phosphate dehydrogenase (GAPDH), Abcam, rabbit polyclonal, WB, 1:2,500, and glyceraldehyde-3 phosphate dehydrogenase; HSV-1 gE, Harvey Friedman, mouse, WB, 1:1,000, and HSV-1 glycoprotein E; AKT, Cell Signaling Technology, rabbit monoclonal, WB, 1:1,000, and protein kinase B; p-AKT, Cell Signaling Technology, rabbit monoclonal, WB, 1:2,000, and phosphorylated protein kinase B; MAP-2, Cell Signaling Technology, rabbit polyclonal, IF, 1:500, and microtubule-associated protein 2; SY38, Abcam, mouse, WB, 1:500, and synaptophysin; GAP-43, Santa Cruz Biotechnology, mouse, WB, 1:1,000, and growth-associated protein 43; IFI-16, David Knipe, mouse monoclonal, IF, 1:50, and IFN- $\gamma$ -inducible protein 16; cGAS, David Knipe, rabbit polyclonal, WB/IF, 1:1,000/1:50, and cyclic GMP-AMP synthase; caspase 3, Cell Signaling Technology, rabbit polyclonal, WB, 1:1,000, inactive, and full-length procaspase 3; SMI-31, Covance, mouse monoclonal, IF, 1:500, and phosphorylated NF-H; SMI-32, Covance, mouse, IF, 1:500, and unphosphorylated NF-H; SV2, Developmental Studies Hybridoma Bank, mouse, IF, 1:250, and synaptic vesicle protein 2; anti-mouse [F(ab')<sub>2</sub>] Alexa Fluor 488, Jackson ImmunoResearch, donkey, IF, 1:200, and secondary antibody—IF; anti-rabbit [F(ab')<sub>2</sub>] Alexa Fluor 647, Jackson ImmunoResearch, donkey, IF, 1:200, and secondary antibody—IF; anti-mouse [F(ab')<sub>2</sub>] Alexa Fluor 647, Jackson ImmunoResearch, donkey, IF, 1:200, and secondary antibody—IF; anti-rabbit [F(ab')<sub>2</sub>] Alexa 488, Jackson ImmunoResearch, donkey, IF, 1:200, and secondary antibody—IF; goat anti-rabbit, Jackson ImmunoResearch, goat, WB, 1:20,000, and secondary antibody—WB; goat anti-mouse, Jackson ImmunoResearch, goat, WB, 1:20,000, and secondary antibody—WB.

**Imaging and immunofluorescence.** Phase-contrast images of uninfected and infected cells were obtained on an inverted epifluorescence microscope (Nikon Eclipse Ti). Images were acquired at a magnification of  $\times 20$  in the bright-field channel. Time-lapse images were taken using an inverted epifluorescence microscope (Nikon Eclipse Ti) with a stage-top incubator (Tokai Hit).

To assess expression and localization of neuronal markers (Fig. 2), undifferentiated SH-SY5Y cells and terminally differentiated SH-SY5Y neuronal cells (53) were grown on ECM-coated glass coverslips. Cells were fixed in 4% paraformaldehyde, rinsed with 1 $\times$  phosphate-buffered saline (PBS), permeabilized with 0.1% Triton X-100–PBS, and blocked with 10% donkey serum (Jackson ImmunoResearch, West Grove, PA) in 0.1% Triton X-100–PBS. Cells were then incubated with primary antibodies (see “Antibodies” above) diluted in 10% donkey serum–0.1% Triton X-100–PBS overnight at 4°C. Coverslips were washed with 0.1% Triton X-100–PBS and then incubated with fluorescence-conjugated secondary antibodies (see “Antibodies” above) diluted in 10% donkey serum–0.1% Triton X-100–PBS for 2 h at room temperature. Cells were washed with 0.1% Triton X-100–PBS, rinsed three times with PBS, and then mounted using ProLong Gold plus 4',6-diamidino-2-phenylindole (DAPI) antifade mounting reagent (Invitrogen).

Assessments of expression and localization of the immune mediators IFI16 and cGAS (Fig. 6) were performed as previously described (20). Briefly, MRC5 fibroblasts and terminally differentiated SH-SY5Y neuronal cells (53) were infected at an MOI of 10 with HSV-1 McKrae in a total volume of 400  $\mu$ l and fixed in 2% paraformaldehyde at 3 hpi or 6 hpi (neuronal cells only). All wash steps and incubations in primary and secondary antibodies were performed as described above, with the use of Hoechst nuclear stain (1:10,000) diluted in 10% donkey serum–0.1% Triton X-100–PBS. Coverslips were then mounted on slides with ProLong Gold antifade reagent (Invitrogen).

All fluorescence images were acquired using an Olympus FV10i confocal microscope with a 60 $\times$  objective and digital zoom as indicated in the text and figure legends. Each image is presented as a maximum projection with background subtraction performed in ImageJ (rolling ball radii = 50 for neuronal cells and 80 for MRC5 cells). Brightness and contrast were adjusted equally for each figure in Adobe Photoshop. To compare expression and localization of neuronal markers, identical laser settings were applied for each SH-SY5Y image pairing (Fig. 2).

**Western blotting.** Soluble protein was separated from total cell lysate as previously described (102). Briefly, cells were lysed using radioimmunoprecipitation assay (RIPA) buffer (Sigma-Aldrich) supplemented with Pierce protease and phosphatase inhibitor minitables (Thermo Scientific). Cells were scraped and combined and then sonicated in a cup holder at 80% amplitude for 4 s on/off using a Q500 ultrasonic processor. Lysates were rocked for 15 min at 4°C and centrifuged at 12,500  $\times g$  for 10 min at 4°C. Supernatant was collected and total protein was quantified using a bicinchoninic acid (BCA) assay (Thermo Scientific) on a NanoDrop 2000c spectrophotometer.

Twenty micrograms of protein from each sample was resolved in 7.5 to 15% sodium dodecyl sulfate-polyacrylamide gel electrophoresis (SDS-PAGE) minigels (Miniprotean; Bio-Rad) and transferred to a 0.45- $\mu$ m or 0.20- $\mu$ m nitrocellulose membrane (Amersham GE Healthcare) using a Trans-Blot SD semidry electrophoresis transfer cell (Bio-Rad) at 15 V for 17 to 25 min. Membranes were blocked in either 5% nonfat dry milk or 3% bovine serum albumin (BSA) prepared in Tris-buffered saline (1 M, pH 7.4), 154 mM NaCl, and 0.2% Tween 20 (TBS-T buffer) for 1 h at room temperature. Primary antibodies were diluted in either 1% milk plus TBS-T or 3% BSA plus TBS-T and incubated overnight at 4°C (see “Antibodies” above). Membranes were washed three times with TBS-T buffer for 20 min each time and then incubated in a 1:20,000 dilution of species-appropriate secondary antibody in either 1% milk plus TBS-T or 3% BSA plus TBS-T for 1 h at room temperature (see “Antibodies” above). Membranes were washed as described above and visualized using enhanced chemiluminescence substrate, SuperSignal West Pico substrate, or SuperSignal West Dura substrate (Thermo Scientific).

For infected-cell Western blots, the above-described protocol was repeated following initial infection with an MOI of 10 using HSV-1 McKrae. Following the infection procedure detailed above, the inoculum was aspirated and replaced with cell-appropriate medium. Pairs of uninfected and infected cell lysates were harvested at 6 hpi.

To assess activation of the caspase cascade and subsequent apoptosis in neuronal SH-SY5Y cells and the epithelial progenitor cells, we examined cleavage of procaspase 3 protein by Western blotting (Fig. 4B). As a positive control for procaspase 3 cleavage, we induced osmotic shock by treating cells with 1.5 M sorbitol for 1 h, followed by 2 h of incubation at 37°C, as previously described (103).

Protein expression levels were quantified using ImageQuant TL8.1 software (GE Healthcare Life Sciences). Regions of interest were drawn around each sample lane, and then rolling-ball subtraction was used to eliminate background signal. The size of the rolling ball used for background subtraction on all Western blot replicates was between 55 and 70 on a parameter scale of 0 to 10,000. Total protein expression present in each sample lane was determined, and each biological replicate for all protein targets of interest was normalized to the matched GAPDH loading control lane obtained on the same day. p-AKT levels were normalized to the matched AKT expression levels for each biological replicate. Ratios of each protein of interest to GAPDH expression were plotted for both undifferentiated and differentiated SH-SY5Y cells (Fig. 3B). For infected Western blot quantitation, ratios of each protein of interest to GAPDH were normalized to the uninfected expression levels for each protein of interest (Fig. 3C).

**Single-step and multistep growth curves.** Neuronal cultures were obtained by initial plating of undifferentiated SH-SY5Y cells at a density of 200,000 or 400,000 cells per 35-mm<sup>2</sup> plate. These were differentiated as previously described (45, 46, 53). The average number of neuronal cells obtained following the 2.5-week differentiation procedure was typically between 30,000 and 100,000 per 35-mm<sup>2</sup> plate. For the single-step growth curve comparison of all three cell types (Fig. 4A), undifferentiated SH-SY5Y cells and SK-N-SH cells were plated 24 h prior to infection at a density of 50,000 or 100,000 per 35-mm<sup>2</sup> plate. On the day of infection, three plates from each cell type were used for cell counting and subsequent virus dilution calculations. Cells were infected at an MOI of 10 and after a 1-h incubation with rocking, the inoculum was replaced and infections were allowed to proceed for 24 h. Both cell-free virus and cell-associated virus were collected during the single round of replication. To harvest the cell-free fraction, medium from infected cells was collected and centrifuged at 1,000 × *g* for 2 min and the supernatant was saved. To collect the cell-associated fraction, infected-cell monolayers were scraped and harvested, resuspended in media, and combined with pelleted cells from the supernatant collection. Both the cell-free and cell-associated samples were freeze-thawed three times prior to determination of virus titers on Vero cells as described above.

For the multistep growth curves (Fig. 5), differentiated SH-SY5Y cells, undifferentiated SH-SY5Y cells, and Vero cells were infected with an MOI of 0.01, with prior counting of three plates to determine the average cell density per plate. Following infection and a 1-h incubation with rocking, the inoculum was replaced with fresh medium containing 0.1% pooled human serum from male AB plasma (Sigma; H4522) and infections were allowed to proceed for 72 h (104, 105). During this time, both cell-free virus and cell-associated virus were collected at 24, 48, and 72 hpi. To harvest the cell-free fraction, medium from infected cells was collected and centrifuged at 5,000 × *g* for 5 min and the supernatant was saved. To collect the cell-associated fraction, infected cell monolayers were scraped and harvested, resuspended in medium, and combined with pelleted cells from the supernatant collection. The samples were thawed, and titers on Vero cells were determined as described above.

## SUPPLEMENTAL MATERIAL

Supplemental material for this article may be found at <https://doi.org/10.1128/JVI.00958-17>.

**SUPPLEMENTAL FILE 1**, MOV file, 9.4 MB.

**SUPPLEMENTAL FILE 2**, MOV file, 5.8 MB.

**SUPPLEMENTAL FILE 3**, PDF file, 0.1 MB.

## ACKNOWLEDGMENTS

We are grateful for the contributions of Yolanda Tafuri in optimizing the conditions for SH-SY5Y cell differentiation and for the support of Lynn Enquist, in whose lab the neuronal differentiation work was initiated. We also thank David Knipe, John Wills, and Harvey Friedman for contributing antibodies to this project. The Sv2 monoclonal antibody developed by Kathleen M. Buckley (Harvard Medical School) was obtained from the Developmental Studies Hybridoma Bank, created by the NIH NICHD and maintained at The University of Iowa in the Department of Biology.

This work was supported by the NIH-NIAID Virus Pathogens Resource (ViPR) Bioinformatics Resource Center (M.L.S.), NIH-NIAID Career Transition Award K22 (AI095384) (M.L.S.), an American Heart Association (AHA) postdoctoral grant (C.A.M.), and research startup funds from the Pennsylvania State University.

The funders had no role in study design, collection and interpretation of data, or the decision to submit this work for publication.

## REFERENCES

- Roizman B, Knipe DM, Whitley R. 2013. Herpes simplex viruses, p 1823–1897. In Knipe DM, Howley PM, Cohen JI, Griffin DE, Lamb RA, Martin MA, Racaniello VR, Roizman B (ed), *Fields virology*, 6th ed. Lippincott Williams & Wilkins, Philadelphia, PA.
- Looker KJ, Magaret AS, May MT, Turner KME, Vickerman P, Gottlieb SL, Newman LM. 2015. Global and regional estimates of prevalent and incident herpes simplex virus type 1 infections in 2012. *PLoS One* 10:e014065. <https://doi.org/10.1371/journal.pone.0140765>.
- Looker KJ, Magaret AS, Turner KME, Vickerman P, Gottlieb SL, Newman LM. 2015. Global estimates of prevalent and incident herpes simplex virus type 2 infections in 2012. *PLoS One* 10:e114989. <https://doi.org/10.1371/journal.pone.0114989>.
- Thompson RL, Preston CM, Sawtell NM. 2009. De novo synthesis of VP16 coordinates the exit from HSV latency in vivo. *PLoS Pathog* 5:e1000352. <https://doi.org/10.1371/journal.ppat.1000352>.
- Wilson AC, Mohr I. 2012. A cultured affair: HSV latency and reactivation neurons. *Trends Microbiol* 20:604–611. <https://doi.org/10.1016/j.tim.2012.08.005>.
- Bloom DC. 2016. Alpha herpesvirus latency: a dynamic state of transcription and reactivation. *Adv Virus Res* 94:53–80. <https://doi.org/10.1016/bs.aivir.2015.10.001>.
- Leib DA, Harrison TE, Laslo KM, Machalek MA, Moorman NJ, Virgin HW. 1999. Interferons regulate the phenotype of wild-type and mutant herpes simplex viruses in vivo. *J Exp Med* 189:663–672. <https://doi.org/10.1084/jem.189.4.663>.
- Dix RD, McKendall RR, Baringer JR. 1983. Comparative neurovirulence of herpes simplex virus type 1 strains after peripheral or intracerebral inoculation of BALB/c mice. *Infect Immun* 40:103–112.
- Whitley RJ, Kimberlin DW, Roizman B. 1998. Herpes simplex viruses. *Clin Infect Dis* 26:541–555. <https://doi.org/10.1086/514600>.
- Knipe DM, Cliffe A. 2008. Chromatin control of herpes simplex virus lytic and latent infection. *Nat Rev Microbiol* 6:211–221. <https://doi.org/10.1038/nrmicro1794>.
- Menachery VD, Pasiaka TJ, Leib DA. 2010. Interferon regulatory factor 3-dependent pathways are critical for control of herpes simplex virus type 1 central nervous system infection. *J Virol* 84:9685–9694. <https://doi.org/10.1128/JVI.00706-10>.
- Kumar H, Kawai T, Akira S. 2011. Pathogen recognition by the innate immune system. *Int Rev Immunol* 30:16–34. <https://doi.org/10.3109/08830185.2010.529976>.
- Sasai M, Yamamoto M. 2013. Pathogen recognition receptors: ligands and signaling pathways by Toll-like receptors. *Int Rev Immunol* 32:116–133. <https://doi.org/10.3109/08830185.2013.774391>.
- Burdette DL, Vance RE. 2013. STING and the innate immune response to nucleic acids in the cytosol. *Nat Immunol* 14:19–26. <https://doi.org/10.1038/ni.2491>.
- Orzalli MH, DeLuca NA, Knipe DM. 2012. Nuclear IFI16 induction of IRF-3 signaling during herpesviral infection and degradation of IFI16 by the viral ICPO protein. *Proc Natl Acad Sci U S A* 109:E3008–E3017. <https://doi.org/10.1073/pnas.1211302109>.
- Sun L, Wu J, Du F, Chen X, Chen ZJ. 2013. Cyclic GMP-AMP synthase is a cytosolic DNA sensor that activates the type I interferon pathway. *Science* 339:786–791. <https://doi.org/10.1126/science.1232458>.
- Li X-D, Wu J, Gao D, Wang H, Sun L, Chen ZJ. 2013. Pivotal roles of cGAS-cGAMP signaling in antiviral defense and immune adjuvant effects. *Science* 341:1390–1394. <https://doi.org/10.1126/science.1244040>.
- Thompson MR, Sharma S, Atianand M, Jensen SB, Carpenter S, Knipe DM, Fitzgerald KA, Kurt-Jones EA. 2014. Interferon-inducible protein (IFI) 16 transcriptionally regulates type I interferons and other interferon-stimulated genes and controls the interferon response to both DNA and RNA viruses. *J Biol Chem* 289:23568–23581. <https://doi.org/10.1074/jbc.M114.554147>.
- Diner BA, Lum KK, Javitt A, Cristea IM. 2015. Interactions of the antiviral factor interferon gamma-inducible protein 16 (IFI16) mediate immune signaling and herpes simplex virus-1 immunosuppression. *Mol Cell Proteomics* 14:2341–2356. <https://doi.org/10.1074/mcp.M114.047068>.
- Orzalli MH, Broekema NM, Diner BA, Hancks DC, Elde NC, Cristea IM, Knipe DM. 2015. cGAS-mediated stabilization of IFI16 promotes innate signaling during herpes simplex virus infection. *Proc Natl Acad Sci U S A* 112:E1773–E1781. <https://doi.org/10.1073/pnas.1424637112>.
- Chen Q, Sun L, Chen ZJ. 2016. Regulation and function of the cGAS-STING pathway of cytosolic DNA sensing. *Nat Immunol* 17:1142–1149. <https://doi.org/10.1038/ni.3558>.
- Jack CS, Arbour N, Manusow J, Montgrain V, Blain M, McCrea E, Shapiro A, Antel JP. 2005. TLR signaling tailors innate immune responses in human microglia and astrocytes. *J Immunol* 175:4320–4330. <https://doi.org/10.4049/jimmunol.175.7.4320>.
- Bsibsi M, Ravid R, Gveric D, van Noort JM. 2002. Broad expression of Toll-like receptors in the human central nervous system. *J Neuropathol Exp Neurol* 61:1013–1021. <https://doi.org/10.1093/jnen/61.11.1013>.
- Lafon M, Megret F, Lafage M, Prehaud C. 2006. The innate immune facet of brain. *J Mol Neurosci* 29:185–194. <https://doi.org/10.1385/JMN:29:3:185>.
- Zhang S-Y, Jouanguy E, Ugolini S, Smahi A, Elain G, Romero P, Segal D, Sancho-Shimizu V, Lorenzo L, Puel A, Picard C, Chappier A, Plancaoulaine S, Titeux M, Cognet C, von Bernuth H, Ku C-L, Casrouge A, Zhang X-X, Barreiro L, Leonard J, Hamilton C, Lebon P, Heron B, Vallee L, Quintana-Murci L, Hovnanian A, Rozenberg F, Vivier E, Geissmann F, Tardieu M, Abel L, Casanova J-L. 2007. TLR3 deficiency in patients with herpes simplex encephalitis. *Science* 317:1522–1527. <https://doi.org/10.1126/science.1139522>.
- Wang T, Town T, Alexopoulou L, Anderson JF, Fikrig E, Flavell RA. 2004. Toll-like receptor 3 mediates West Nile virus entry into the brain causing lethal encephalitis. *Nat Med* 10:1366–1373. <https://doi.org/10.1038/nm1140>.
- Boulangier LM, Shatz CJ. 2004. Immune signalling in neural development, synaptic plasticity and disease. *Nat Rev Neurosci* 5:521–531. <https://doi.org/10.1038/nrn1428>.
- VanGuilder Starkey HD, Van Kirk CA, Bixler GV, Imperio CG, Kale VP, Serfass JM, Farley JA, Yan H, Warrington JP, Han S, Mitschelen M, Sonntag WE, Freeman WM. 2012. Neuroglial expression of the MHCI pathway and PirB receptor is upregulated in the hippocampus with advanced aging. *J Mol Neurosci* 48:111–126. <https://doi.org/10.1007/s12031-012-9783-8>.
- Redwine JA, Buchmeier MJ, Evans CF. 2001. In vivo expression of major histocompatibility complex molecules on oligodendrocytes and neurons during viral infection. *Am J Pathol* 159:1219–1224. [https://doi.org/10.1016/S0002-9440\(10\)62507-2](https://doi.org/10.1016/S0002-9440(10)62507-2).
- Pereira RA, Tschärke DC, Simmons A. 1994. Upregulation of class I major histocompatibility complex gene expression in primary sensory neurons, satellite cells, and Schwann cells of mice in response to acute but not latent herpes simplex virus infection in vivo. *J Exp Med* 180:841–841. <https://doi.org/10.1084/jem.180.3.841>.
- Markus A, Grigoryan S, Sloutskin A, Yee MB, Zhu H, Yang IH, Thakor NV, Sarid R, Kinchington PR, Goldstein RS. 2011. Varicella-zoster virus (VZV) infection of neurons derived from human embryonic stem cells: direct demonstration of axonal infection, transport of VZV, and productive neuronal infection. *J Virol* 85:6220–6233. <https://doi.org/10.1128/JVI.02396-10>.
- De Regge N, Favoreel HW, Geenen K, Nauwynck HJ. 2006. A homologous in vitro model to study interactions between alpha herpesviruses and trigeminal ganglion neurons. *Vet Microbiol* 113:251–255. <https://doi.org/10.1016/j.vetmic.2005.11.004>.
- Trousdale MD, Steiner I, Spivack JG, Deshmane SL, Brown SM, MacLean AR, Subak-Sharpe JH, Fraser NW. 1991. In vivo and in vitro reactivation impairment of a herpes simplex virus type 1 latency-associated transcript variant in a rabbit eye model. *J Virol* 65:6989–6993.
- Kobayashi M, Kim J-Y, Camarena V, Roehm PC, Chao MV, Wilson AC, Mohr I. 2012. A primary neuron culture system for the study of herpes simplex virus latency and reactivation. *J Vis Exp* 2012 (62):3823.
- Brodeur GM, Sekhon G, Goldstein MN. 1977. Chromosomal aberrations in human neuroblastomas. *Cancer* 40:2256–2263. [https://doi.org/10.1002/1097-0142\(197711\)40:5<2256::AID-CNCR2820400536>3.0.CO;2-1](https://doi.org/10.1002/1097-0142(197711)40:5<2256::AID-CNCR2820400536>3.0.CO;2-1).
- Hu B-Y, Weick JP, Yu J, Ma L-X, Zhang X-Q, Thomson JA, Zhang S-C.

2010. Neural differentiation of human induced pluripotent stem cells follows developmental principles but with variable potency. *Proc Natl Acad Sci U S A* 107:4335–4340. <https://doi.org/10.1073/pnas.0910012107>.
37. Cheng Y, Ma Z, Kim B-H, Wu W, Cayting P, Boyle AP, Sundaram V, Xing X, Dogan N, Li J, Euskirchen G, Lin S, Lin Y, Visel A, Kawli T, Yang X, Patacsil D, Keller CA, Giardine B, The Mouse ENCODE Consortium, Kundaje A, Wang T, Pennacchio LA, Weng Z, Hardison RC, Snyder MP. 2014. Principles of regulatory information conservation between mouse and human. *Nature* 515:371–375. <https://doi.org/10.1038/nature13985>.
  38. Lin S, Lin Y, Nery JR, Ulrich MA, Breschi A, Davis CA, Dobin A, Zaleski C, Beer MA, Chapman WC, Gingeras TR, Ecker JR, Snyder MP. 2014. Comparison of the transcriptional landscapes between human and mouse tissues. *Proc Natl Acad Sci U S A* 111:17224–17229. <https://doi.org/10.1073/pnas.1413624111>.
  39. Odom DT, Dowell RD, Jacobsen ES, Gordon W, Danford TW, MacIsaac KD, Rolfe PA, Conboy CM, Gifford DK, Fraenkel E. 2007. Tissue-specific transcriptional regulation has diverged significantly between human and mouse. *Nat Genet* 39:730–732. <https://doi.org/10.1038/ng2047>.
  40. McGeoch DJ, Cook S. 1994. Molecular phylogeny of the alphaherpesvirinae subfamily and a proposed evolutionary timescale. *J Mol Biol* 238:9–22.
  41. Whitley RJ. 2006. Herpes simplex encephalitis: adolescents and adults. *Antiviral Res* 71:141–148. <https://doi.org/10.1016/j.antiviral.2006.04.002>.
  42. Whitley RJ. 2015. Herpes simplex virus infections of the central nervous system. *Contin Lifelong Learn Neurol* 21:1704–1713. <https://doi.org/10.1212/CON.0000000000000243>.
  43. Sancho-Shimizu V, Zhang S-Y, Abel L, Tardieu M, Rozenberg F, Jouanguy E, Casanova J-L. 2007. Genetic susceptibility to herpes simplex virus 1 encephalitis in mice and humans. *Curr Opin Allergy Clin Immunol* 7:495–505. <https://doi.org/10.1097/ACI.0b013e3282f151d2>.
  44. Kastrukoff LF, Lau AS, Thomas EE. 2012. The effect of mouse strain on herpes simplex virus type 1 (HSV-1) infection of the central nervous system (CNS). *Herpesviridae* 3:4. <https://doi.org/10.1186/2042-4280-3-4>.
  45. Encinas M, Iglesias M, Liu Y, Wang H, Muhaisen A, Ceña V, Gallego C, Comella JX. 2000. Sequential treatment of SH-SY5Y cells with retinoic acid and brain-derived neurotrophic factor gives rise to fully differentiated, neurotrophic factor-dependent, human neuron-like cells. *J Neurochem* 75:991–1003. <https://doi.org/10.1046/j.1471-4159.2000.0750991.x>.
  46. Christensen J, Steain M, Slobedman B, Abendroth A. 2011. Differentiated neuroblastoma cells provide a highly efficient model for studies of productive varicella-zoster virus infection of neuronal cells. *J Virol* 85:8436–8442. <https://doi.org/10.1128/JVI.00515-11>.
  47. Biedler JL, Helson L, Spengler BA. 1973. Morphology and growth, tumorigenicity, and cytogenetics of human neuroblastoma cells in continuous culture. *Cancer Res* 33:2643–2652.
  48. Gimenez-Cassina A, Lim F, Diaz-Nido J. 2006. Differentiation of a human neuroblastoma into neuron-like cells increases their susceptibility to transduction by herpesviral vectors. *J Neurosci Res* 84:755–767. <https://doi.org/10.1002/jnr.20976>.
  49. Allsopp TE, McLuckie J, Kerr LE, Macleod M, Sharkey J, Kelly JS. 2000. Caspase 6 activity initiates caspase 3 activation in cerebellar granule cell apoptosis. *Cell Death Differ* 7:984–993. <https://doi.org/10.1038/sj.cdd.4400733>.
  50. Schamberger CJ, Gerner C, Cerni C. 2005. Caspase-9 plays a marginal role in serum starvation-induced apoptosis. *Exp Cell Res* 302:115–128. <https://doi.org/10.1016/j.yexcr.2004.08.026>.
  51. Pählman S, Hoehner JC, Nånberg E, Hedborg F, Fagerström S, Gestblom C, Johansson I, Larsson U, Lavenius E, Örtoft E, Söderholm H. 1995. Differentiation and survival influences of growth factors in human neuroblastoma. *Eur J Cancer* 31:453–458. [https://doi.org/10.1016/0959-8049\(95\)00033-F](https://doi.org/10.1016/0959-8049(95)00033-F).
  52. Patapoutian A, Reichardt LF. 2001. Trk receptors: mediators of neurotrophin action. *Curr Opin Neurobiol* 11:272–280. [https://doi.org/10.1016/S0959-4388\(00\)00208-7](https://doi.org/10.1016/S0959-4388(00)00208-7).
  53. Shipley MM, Mangold CA, Szpara ML. 2016. Differentiation of the SH-SY5Y human neuroblastoma cell line. *J Vis Exp* 2016 (108):e53193.
  54. Yang M-R, Lee SR, Oh W, Lee E-W, Yeh J-Y, Nah J-J, Joo Y-S, Shin J, Lee H-W, Pyo S, Song J. 2008. West Nile virus capsid protein induces p53-mediated apoptosis via the sequestration of HDM2 to the nucleus. *Cell Microbiol* 10:165–176. <https://doi.org/10.1111/j.1462-5822.2007.01081.x>.
  55. La Monica N, Racaniello VR. 1989. Differences in replication of attenuated and neurovirulent polioviruses in human neuroblastoma cell line SH-SY5Y. *J Virol* 63:2357–2360.
  56. Castorena KM, Peltier DC, Peng W, Miller DJ. 2008. Maturation-dependent responses of human neuronal cells to western equine encephalitis virus infection and type I interferons. *Virology* 372: 208–220. <https://doi.org/10.1016/j.virol.2007.10.025>.
  57. Irwin DJ, Wunner WH, Ertl HC, Jackson AC. 1999. Basis of rabies virus neurovirulence in mice: expression of major histocompatibility complex class I and class II mRNAs. *J Neurovirol* 5:485–494. <https://doi.org/10.3109/13550289909045377>.
  58. Constantinescu R, Constantinescu AT, Reichmann H, Janetzky B. 2007. Neuronal differentiation and long-term culture of the human neuroblastoma line SH-SY5Y. *J Neural Transm Suppl* 72:17–28. [https://doi.org/10.1007/978-3-211-73574-9\\_3](https://doi.org/10.1007/978-3-211-73574-9_3).
  59. Cheung Y-T, Lau WK-W, Yu M-S, Lai CS-W, Yeung S-C, So K-F, Chang RC-C. 2009. Effects of all-trans-retinoic acid on human SH-SY5Y neuroblastoma as in vitro model in neurotoxicity research. *Neurotoxicology* 30:127–135. <https://doi.org/10.1016/j.neuro.2008.11.001>.
  60. Nixon Ralph A, Sihag Ram K. 1991. Neurofilament phosphorylation: a new look at regulation and function. *Trends Neurosci* 14:501–506.
  61. Nowack A, Yao J, Custer KL, Bajjalieh SM. 2010. SV2 regulates neurotransmitter release via multiple mechanisms. *Am J Physiol Cell Physiol* 299:C960–C967. <https://doi.org/10.1152/ajpcell.00259.2010>.
  62. Benowitz LI, Routtenberg A. 1987. A membrane phosphoprotein associated with neural development, axonal regeneration, phospholipid metabolism, and synaptic plasticity. *Trends Neurosci* 10:527–531. [https://doi.org/10.1016/0166-2236\(87\)90135-4](https://doi.org/10.1016/0166-2236(87)90135-4).
  63. Wiedenmann B, Franke WW, Kuhn C, Moll R, Gould VE. 1986. Synaptophysin: a marker protein for neuroendocrine cells and neoplasms. *Proc Natl Acad Sci U S A* 83:3500–3504. <https://doi.org/10.1073/pnas.83.10.3500>.
  64. Reference deleted.
  65. Camarena V, Kobayashi M, Kim JY, Roehm P, Perez R, Gardner J, Wilson AC, Mohr I, Chao MV. 2010. Nature and duration of growth factor signaling through receptor tyrosine kinases regulates HSV-1 latency in neurons. *Cell Host Microbe* 8:320–330. <https://doi.org/10.1016/j.chom.2010.09.007>.
  66. Ma Z, Damania B. 2016. The cGAS-STING defense pathway and its counteraction by viruses. *Cell Host Microbe* 19:150–158. <https://doi.org/10.1016/j.chom.2016.01.010>.
  67. Williams LE, Nesburn AB, Kaufman HE. 1965. Experimental induction of disciform keratitis. *Arch Ophthalmol* 73:112–114. <https://doi.org/10.1001/archophth.1965.00970030114023>.
  68. Hill JM, Radfield MA, Haruta Y. 1987. Strain specificity of spontaneous and adrenergically induced HSV-1 ocular reactivation in latently infected rabbits. *Curr Eye Res* 6:91–97. <https://doi.org/10.3109/02713688709020074>.
  69. Wang H, Davido DJ, Morrison LA. 2013. HSV-1 strain McKrae is more neuroinvasive than HSV-1 KOS after corneal or vaginal inoculation in mice. *Virus Res* 173:436–440. <https://doi.org/10.1016/j.virusres.2013.01.001>.
  70. Sedarati F, Stevens JG. 1987. Biological basis for virulence of three strains of herpes simplex virus type 1. *J Gen Virol* 68:2389–2395. <https://doi.org/10.1099/0022-1317-68-9-2389>.
  71. Khodarev NN, Advani SJ, Gupta N, Roizman B, Weichselbaum RR. 1999. Accumulation of specific RNAs encoding transcriptional factors and stress response proteins against a background of severe depletion of cellular RNAs in cells infected with herpes simplex virus 1. *Proc Natl Acad Sci U S A* 96:12062–12067. <https://doi.org/10.1073/pnas.96.21.12062>.
  72. Bellacosa A, Testa JR, Staal SP, Tschlis PN. 1991. A retroviral oncogene, akt, encoding a serine-threonine kinase containing an SH2-like region. *Science* 254:274–277. <https://doi.org/10.1126/science.1833819>.
  73. Franke TF, Yang S, Chan TO, Datta K, Kazlauskas A, Morrison DK, Kaplan DR, Tschlis PN. 1995. The protein kinase encoded by the akt proto-oncogene is a target of the PDGF-activated phosphatidylinositol 3-kinase. *Cell* 81: 727–736. [https://doi.org/10.1016/0092-8674\(95\)90534-0](https://doi.org/10.1016/0092-8674(95)90534-0).
  74. Qiao J, Paul P, Lee S, Qiao L, Josifi E, Tiao JR, Chung DH. 2012. PI3K/AKT and ERK regulate retinoic acid-induced neuroblastoma cellular differentiation. *Biochem Biophys Res Commun* 424:421–426. <https://doi.org/10.1016/j.bbrc.2012.06.125>.
  75. Kaplan DR, Matsumoto K, Lucarelli E, Thiele CJ. 1993. Induction of TrkB by retinoic acid mediates biologic responsiveness to BDNF and differ-



- entiation of human neuroblastoma cells. *Neuron* 11:321–331. [https://doi.org/10.1016/0896-6273\(93\)90187-V](https://doi.org/10.1016/0896-6273(93)90187-V).
76. Benetti L, Roizman B. 2006. Protein kinase B/Akt is present in activated form throughout the entire replicative cycle of deltaU(S)3 mutant virus but only at early times after infection with wild-type herpes simplex virus 1. *J Virol* 80:3341–3348. <https://doi.org/10.1128/JVI.80.7.3341-3348.2006>.
  77. Cheshenko N, Trepanier JB, Stefanidou M, Buckley N, Gonzalez P, Jacobs W, Herold BC. 2013. HSV activates Akt to trigger calcium release and promote viral entry: novel candidate target for treatment and suppression. *FASEB J* 27:2584–2599. <https://doi.org/10.1096/fj.12-220285>.
  78. Liu X, Cohen JL. 2015. The role of PI3K/Akt in human herpesvirus infection: from the bench to the bedside. *Virology* 479–480:568–577.
  79. Datta SR, Dudek H, Tao X, Masters S, Fu H, Gotoh Y, Greenberg ME. 1997. Akt phosphorylation of BAD couples survival signals to the cell-intrinsic death machinery. *Cell* 91:231–241. [https://doi.org/10.1016/S0092-8674\(00\)80405-5](https://doi.org/10.1016/S0092-8674(00)80405-5).
  80. Manning BD, Cantley LC. 2007. AKT/PKB signaling: navigating downstream. *Cell* 129:1261–1274. <https://doi.org/10.1016/j.cell.2007.06.009>.
  81. Kaur S, Sassano A, Dolniak B, Joshi S, Majchrzak-Kita B, Baker DP, Hay N, Fish EN, Platanius LC. 2008. Role of the Akt pathway in mRNA translation of interferon-stimulated genes. *Proc Natl Acad Sci U S A* 105:4808–4813. <https://doi.org/10.1073/pnas.0710907105>.
  82. Buchkovich NJ, Yu Y, Zampieri CA, Alwine JC. 2008. The TORrid affairs of viruses: effects of mammalian DNA viruses on the PI3K-Akt-mTOR signalling pathway. *Nat Rev Microbiol* 6:266–275. <https://doi.org/10.1038/nrmicro1855>.
  83. Tiwari V, Shukla D. 2010. Phosphoinositide 3 kinase signalling may affect multiple steps during herpes simplex virus type-1 entry. *J Gen Virol* 91:3002–3009. <https://doi.org/10.1099/vir.0.024166-0>.
  84. Kobayashi M, Wilson AC, Chao MV, Mohr I. 2012. Control of viral latency in neurons by axonal mTOR signaling and the 4E-BP translation repressor. *Genes Dev* 26:1527–1532. <https://doi.org/10.1101/gad.190157.112>.
  85. Chuluunbaatar U, Mohr I. 2011. A herpesvirus kinase that masquerades as Akt: you don't have to look like Akt, to act like it. *Cell Cycle* 10:2064–2068. <https://doi.org/10.4161/cc.10.13.16242>.
  86. Tao J, Zhou X, Jiang Z. 2016. cGAS-cGAMP-STING: the three musketeers of cytosolic DNA sensing and signaling: cytosolic DNA sensing and signaling. *IUBMB Life* 68:858–870. <https://doi.org/10.1002/iub.1566>.
  87. Seo JJ, Yang A, Tan B, Kim S, Liang Q, Choi Y, Yuan W, Feng P, Park H-S, Jung JU. 2015. Akt kinase-mediated checkpoint of cGAS DNA sensing pathway. *Cell Rep* 13:440–449. <https://doi.org/10.1016/j.celrep.2015.09.007>.
  88. Sawtell NM, Poon DK, Tansky CS, Thompson RL. 1998. The latent herpes simplex virus type 1 genome copy number in individual neurons is virus strain specific and correlates with reactivation. *J Virol* 72:5343–5350.
  89. Luker KE, Schultz T, Romine J, Leib DA, Luker GD. 2006. Transgenic reporter mouse for bioluminescence imaging of herpes simplex virus 1 infection in living mice. *Virology* 347:286–295. <https://doi.org/10.1016/j.virol.2005.12.016>.
  90. Lyman MG, Kemp CD, Taylor MP, Enquist LW. 2009. Comparison of the pseudorabies virus Us9 protein with homologs from other veterinary and human alphaherpesviruses. *J Virol* 83:6978–6986. <https://doi.org/10.1128/JVI.00598-09>.
  91. Negatsch A, Mettenleiter TC, Fuchs W. 2011. Herpes simplex virus type 1 strain KOS carries a defective US9 and a mutated US8A gene. *J Gen Virol* 92:167–172. <https://doi.org/10.1099/vir.0.026484-0>.
  92. Howard PW, Howard TL, Johnson DC. 2013. Herpes simplex virus membrane proteins gE/gL and US9 act cooperatively to promote transport of capsids and glycoproteins from neuron cell bodies into initial axon segments. *J Virol* 87:403–414. <https://doi.org/10.1128/JVI.02465-12>.
  93. Sawtell NM, Thompson RL. 2016. De novo herpes simplex virus VP16 expression gates a dynamic programmatic transition and sets the latent/lytic balance during acute infection in trigeminal ganglia. *PLoS Pathog* 12:e1005877. <https://doi.org/10.1371/journal.ppat.1005877>.
  94. Hamza MA, Higgins DM, Ruyechan WT. 2006. Herpes simplex virus type-1 latency inhibits dendritic growth in sympathetic neurons. *Neurobiol Dis* 24:367–373. <https://doi.org/10.1016/j.nbd.2006.07.011>.
  95. Danaher RJ, McGarrell BS, Stromberg AJ, Miller CS. 2008. Herpes simplex virus type 1 modulates cellular gene expression during quiescent infection of neuronal cells. *Arch Virol* 153:1335–1345. <https://doi.org/10.1007/s00705-008-0122-x>.
  96. Roehm PC, Camarena V, Nayak S, Gardner JB, Wilson A, Mohr I, Chao MV. 2011. Cultured vestibular ganglion neurons demonstrate latent HSV1 reactivation. *Laryngoscope* 121:2268–2275. <https://doi.org/10.1002/lary.22035>.
  97. Mattila RK, Harila K, Kangas SM, Paavilainen H, Heape AM, Mohr IJ, Hukkanen V. 2015. An investigation of herpes simplex virus type 1 latency in a novel mouse dorsal root ganglion model suggests a role for ICP34.5 in reactivation. *J Gen Virol* 96:2304–2313. <https://doi.org/10.1099/vir.0.000138>.
  98. Pourchet A, Modrek A, Placantonakis D, Mohr I, Wilson A. 2017. Modeling HSV-1 latency in human embryonic stem cell-derived neurons. *Pathogens* 6:24. <https://doi.org/10.3390/pathogens6020024>.
  99. Macdonald SJ, Mostafa HH, Morrison LA, Davido DJ. 2012. Genome sequence of herpes simplex virus 1 strain McKrae. *J Virol* 86:9540–9541. <https://doi.org/10.1128/JVI.01469-12>.
  100. Bowen CD, Renner DW, Shreve JT, Tafuri Y, Payne KM, Dix RD, Kinchington PR, Gatherer D, Szpara ML. 2016. Viral forensic genomics reveals the relatedness of classic herpes simplex virus strains KOS, KOS63, and KOS79. *Virology* 492:179–186. <https://doi.org/10.1016/j.virol.2016.02.013>.
  101. Antinone SE, Smith GA. 2010. Retrograde axon transport of herpes simplex virus and pseudorabies virus: a live-cell comparative analysis. *J Virol* 84:1504–1512. <https://doi.org/10.1128/JVI.02029-09>.
  102. VanGuilder HD, Yan H, Farley JA, Sonntag WE, Freeman WM. 2010. Aging alters the expression of neurotransmission-regulating proteins in the hippocampal synaptosome. *J Neurochem* 113:1577–1588.
  103. Galvan V, Brandimarti R, Roizman B. 1999. Herpes simplex virus 1 blocks caspase-3-independent and caspase-dependent pathways to cell death. *J Virol* 73:3219–3226.
  104. Dingwell KS, Brunetti CR, Hendricks RL, Tang Q, Tang M, Rainbow AJ, Johnson DC. 1994. Herpes simplex virus glycoproteins E and I facilitate cell-to-cell spread in vivo and across junctions of cultured cells. *J Virol* 68:834–845.
  105. Pasiaka TJ, Lu B, Crosby SD, Wylie KM, Morrison LA, Alexander DE, Menachery VD, Leib DA. 2008. Herpes simplex virus virion host shutoff attenuates establishment of the antiviral state. *J Virol* 82:5527–5535. <https://doi.org/10.1128/JVI.02047-07>.
  106. Nicola AV, Hou J, Major EO, Straus SE. 2005. Herpes simplex virus type 1 enters human epidermal keratinocytes, but not neurons, via a pH-dependent endocytic pathway. *J Virol* 79:7609–7616. <https://doi.org/10.1128/JVI.79.12.7609-7616.2005>.
  107. Kato A, Hirohata Y, Arai J, Kawaguchi Y. 2014. Phosphorylation of herpes simplex virus 1 dUTPase upregulated viral dUTPase activity to compensate for low cellular dUTPase activity for efficient viral replication. *J Virol* 88:7776–7785. <https://doi.org/10.1128/JVI.00603-14>.
  108. Galvan V, Roizman B. 1998. Herpes simplex virus 1 induces and blocks apoptosis at multiple steps during infection and protects cells from exogenous inducers in a cell-type-dependent manner. *Proc Natl Acad Sci U S A* 95:3931–3936.
  109. Xiang Y, Zheng K, Ju H, Wang S, Pei Y, Ding W, Chen Z, Wang Q, Qiu X, Zhong M, Zeng F, Ren Z, Qian C, Liu G, Kitazato K, Wang Y. 2012. Cofilin 1-mediated biphasic F-actin dynamics of neuronal cells affect herpes simplex virus 1 infection and replication. *J Virol* 86:8440–8451. <https://doi.org/10.1128/JVI.00609-12>.
  110. Peng W, Henderson G, Inman M, BenMohamed L, Perng G-C, Wechsler SL, Jones C. 2005. The locus encompassing the latency-associated transcript of herpes simplex virus type 1 interferes with and delays interferon expression in productively infected neuroblastoma cells and trigeminal ganglia of acutely infected mice. *J Virol* 79:6162–6171. <https://doi.org/10.1128/JVI.79.10.6162-6171.2005>.
  111. Lafon M, Prehaud C, Megret F, Lafage M, Mouillot G, Roa M, Moreau P, Rouas-Freiss N, Carosella ED. 2005. Modulation of HLA-G expression in human neural cells after neurotropic viral infections. *J Virol* 79:15226–15237. <https://doi.org/10.1128/JVI.79.24.15226-15237.2005>.
  112. Zhou G, Galvan V, Campadelli-Fiume G, Roizman B. 2000. Glycoprotein D or J delivered in *trans* blocks apoptosis in SK-N-SH cells induced by a herpes simplex virus 1 mutant lacking intact genes expressing both glycoproteins. *J Virol* 74:11782–11791. <https://doi.org/10.1128/JVI.74.24.11782-11791.2000>.
  113. Härle P, Sainz B, Carr DJ, Halford WP. 2002. The immediate-early protein, ICP0, is essential for the resistance of herpes simplex virus to interferon- $\alpha/\beta$ . *Virology* 293:295–304. <https://doi.org/10.1006/viro.2001.1280>.
  114. Lagunoff M, Randall G, Roizman B. 1996. Phenotypic properties of

- herpes simplex virus 1 containing a derepressed open reading frame P gene. *J Virol* 70:1810–1817.
115. Snyder A, Wisner TW, Johnson DC. 2006. Herpes simplex virus capsids are transported in neuronal axons without an envelope containing the viral glycoproteins. *J Virol* 80:11165–11177. <https://doi.org/10.1128/JVI.01107-06>.
  116. Wisner TW, Sugimoto K, Howard PW, Kawaguchi Y, Johnson DC. 2011. Anterograde transport of herpes simplex virus capsids in neurons by both separate and married mechanisms. *J Virol* 85:5919–5928. <https://doi.org/10.1128/JVI.00116-11>.
  117. Shinohara T, Nagashima K, Major EO. 1997. Propagation of the human polyomavirus, JCV, in human neuroblastoma cell lines. *Virology* 228:269–277.
  118. Zhuo B, Wang R, Yin Y, Zhang H, Ma T, Liu F, Cao H, Shi Y. 2013. Adenovirus arming human IL-24 inhibits neuroblastoma cell proliferation in vitro and xenograft tumor growth in vivo. *Tumor Biol* 34:2419–2426. <https://doi.org/10.1007/s13277-013-0792-1>.
  119. Jha HC, Mehta D, Lu J, El-Naccache D, Shukla SK, Kovacsics C, Kolson D, Robertson ES. 2015. Gammaherpesvirus infection of human neuronal cells. *mBio* 6:e01844-15. <https://doi.org/10.1128/mBio.01844-15>.
  120. Ahmed M, Lock M, Miller CG, Fraser NW. 2002. Regions of the herpes simplex virus type 1 latency-associated transcript that protect cells from apoptosis in vitro and protect neuronal cells in vivo. *J Virol* 76:717–729. <https://doi.org/10.1128/JVI.76.2.717-729.2002>.
  121. Kang W, Mukerjee R, Fraser NW. 2003. Establishment and maintenance of HSV latent infection is mediated through correct splicing of the LAT primary transcript. *Virology* 312:233–244. [https://doi.org/10.1016/S0042-6822\(03\)00201-0](https://doi.org/10.1016/S0042-6822(03)00201-0).
  122. De Chiara G, Marocci ME, Civitelli L, Argnani R, Piacentini R, Ripoli C, Manservigi R, Grassi C, Garaci E, Palamara AT. 2010. APP processing induced by herpes simplex virus type 1 (HSV-1) yields several APP fragments in human and rat neuronal cells. *PLoS One* 5:e13989. <https://doi.org/10.1371/journal.pone.0013989>.
  123. Gupta A, Gartner JJ, Sethupathy P, Hatzigeorgiou G, Fraser NW. 2006. Anti-apoptotic function of a microRNA encoded by the HSV-1 latency-associated transcript. *Nature* 442:82–85.
  124. Thomas DL, Lock M, Zabolotny JM, Mohan BR, Fraser NW. 2002. The 2-kilobase intron of the herpes simplex virus type 1 latency-associated transcript has a half-life of approximately 24 hours in SY5Y and COS-1 cells. *J Virol* 76:532–540. <https://doi.org/10.1128/JVI.76.2.532-540.2002>.
  125. Xu K, Liu X-N, Zhang H-B, An N, Wang Y, Zhang Z-C, Wang Y-N. 2014. Replication-defective HSV-1 effectively targets trigeminal ganglion and inhibits viral pathogenesis by mediating interferon gamma expression in SH-SY5Y cells. *J Mol Neurosci* 53:78–86. <https://doi.org/10.1007/s12031-013-0199-x>.
  126. Cho H-J, Song MJ. 2014. A gammaherpesvirus establishes persistent infection in neuroblastoma cells. *Mol Cells* 37:518–525. <https://doi.org/10.14348/molcells.2014.0024>.
  127. Thunuguntla P, El-mayet FS, Jones C. 2017. Bovine herpesvirus 1 can efficiently infect the human (SH-SY5Y) but not the mouse neuroblastoma cell line (Neuro-2A). *Virus Res* 232:1–5. <https://doi.org/10.1016/j.virusres.2017.01.011>.
  128. Christensen J, Steain M, Slobedman B, Abendroth A. 2013. Varicella-zoster virus glycoprotein I is essential for spread in dorsal root ganglia and facilitates axonal localization of structural virion components in neuronal cultures. *J Virol* 87:13719–13728. <https://doi.org/10.1128/JVI.02293-13>.
  129. Carbone KM, Rubin SA, Sierra-Honigsmann AM, Lederman HM. 1993. Characterization of a glial cell line persistently infected with Borna disease virus (BDV): influence of neurotrophic factors on BDV protein and RNA expression. *J Virol* 67:1453–1460.
  130. Jan J-T, Chen B-H, Ma S-H, Liu C-I, Tsai H-P, Wu H-C, Jiang S-Y, Yang K-D, Shiao M-F. 2000. Potential dengue virus-triggered apoptotic pathway in human neuroblastoma cells: arachidonic acid, superoxide anion, and NF- $\kappa$ B are sequentially involved. *J Virol* 74:8680–8691. <https://doi.org/10.1128/JVI.74.18.8680-8691.2000>.
  131. Tung W-H, Hsieh H-L, Lee I-T, Yang C-M. 2011. Enterovirus 71 induces integrin  $\beta$ 1/EGFR-Rac1-dependent oxidative stress in SK-N-SH cells: role of HO-1/CO in viral replication. *J Cell Physiol* 226:3316–3329. <https://doi.org/10.1002/jcp.22677>.
  132. Takamatsu Y, Uchida L, Morita K. 2015. Delayed IFN response differentiates replication of West Nile virus and Japanese encephalitis virus in human neuroblastoma and glioblastoma cells. *J Gen Virol* 96:2194–2199. <https://doi.org/10.1099/vir.0.000168>.
  133. Dou J, Daly J, Yuan Z, Jing T, Solomon T. 2009. Bacterial cell surface display: a method for studying Japanese encephalitis virus pathogenicity. *Jpn J Infect Dis* 62:402–408.
  134. Zhang S-C, Cai W-S, Zhang Y, Jiang K-L, Zhang K-R, Wang W-L. 2012. Engineered measles virus Edmonston strain used as a novel oncolytic viral system against human neuroblastoma through a CD46 and nectin 4-independent pathway. *Cancer Lett* 325:227–237. <https://doi.org/10.1016/j.canlet.2012.07.008>.
  135. Shingai M. 2003. Receptor use by vesicular stomatitis virus pseudotypes with glycoproteins of defective variants of measles virus isolated from brains of patients with subacute sclerosing panencephalitis. *J Gen Virol* 84:2133–2143. <https://doi.org/10.1099/vir.0.19091-0>.
  136. Ishida H, Ayata M, Shingai M, Matsunaga I, Seto Y, Katayama Y, Iritani N, Seya T, Yanagi Y, Matsuoka O, Yamano T, Ogura H. 2004. Infection of different cell lines of neural origin with subacute sclerosing panencephalitis (SSPE) virus. *Microbiol Immunol* 48:277–287. <https://doi.org/10.1111/j.1348-0421.2004.tb03524.x>.
  137. Shimada S, Aoki K, Nabeshima T, Fuxun Y, Kurosaki Y, Shioyama K, Onouchi T, Sakaguchi M, Fuchigami T, Ono H, Nishi K, Posadas-Herrera G, Uchida L, Takamatsu Y, Yasuda J, Tsutsumi Y, Fujita H, Morita K, Hayasaka D. 2016. Tofla virus: a newly identified *Nairovirus* of the Crimean-Congo hemorrhagic fever group isolated from ticks in Japan. *Sci Rep* 6:20213. <https://doi.org/10.1038/srep20213>.
  138. Laassri M, Bidzhieva B, Speicher J, Pletnev AG, Chumakov K. 2011. Microarray hybridization for assessment of the genetic stability of chimeric West Nile/dengue 4 virus. *J Med Virol* 83:910–920. <https://doi.org/10.1002/jmv.22033>.
  139. Xu L-J, Jiang T, Zhang F-J, Han J-F, Liu J, Zhao H, Li X-F, Liu R-J, Deng Y-Q, Wu X-Y, Zhu S-Y, Qin E-D, Qin C-F. 2013. Global transcriptomic analysis of human neuroblastoma cells in response to enterovirus type 71 infection. *PLoS One* 8:e65948. <https://doi.org/10.1371/journal.pone.0065948>.
  140. Du X, Wang H, Xu F, Huang Y, Liu Z, Liu T. 2015. Enterovirus 71 induces apoptosis of SH-SY5Y human neuroblastoma cells through stimulation of endogenous microRNA let-7b expression. *Mol Med Rep* 12:953–959. <https://doi.org/10.3892/mmr.2015.3482>.
  141. Bardi G, Sengupta R, Khan MZ, Patel JP, Meucci O. 2006. Human immunodeficiency virus gp120-induced apoptosis of human neuroblastoma cells in the absence of CXCR4 internalization. *J Neurovirol* 12:211–218. <https://doi.org/10.1080/13550280600848373>.
  142. Khan MB, Lang MJ, Huang M-B, Raymond A, Bond VC, Shiramizu B, Powell MD. 2016. Nef exosomes isolated from the plasma of individuals with HIV-associated dementia (HAD) can induce A $\beta$ 1-42 secretion in SH-SY5Y neural cells. *J Neurovirol* 22:179–190. <https://doi.org/10.1007/s13365-015-0383-6>.
  143. Hu L, Uzhameckis D, Hedborg F, Blomberg J. 2016. Dynamic and selective HERV RNA expression in neuroblastoma cells subjected to variation in oxygen tension and demethylation. *APMIS* 124:140–149. <https://doi.org/10.1111/apm.12494>.
  144. Song B-H, Yun G-N, Kim J-K, Yun S-I, Lee Y-M. 2012. Biological and genetic properties of SA14-14-2, a live-attenuated Japanese encephalitis vaccine that is currently available for humans. *J Microbiol* 50:698–706. <https://doi.org/10.1007/s12275-012-2336-6>.
  145. Kim J-M, Yun S-I, Song B-H, Hahn Y-S, Lee C-H, Oh H-W, Lee Y-M. 2008. A single N-linked glycosylation site in the Japanese encephalitis virus prM protein is critical for cell type-specific prM protein biogenesis, virus particle release, and pathogenicity in mice. *J Virol* 82:7846–7862. <https://doi.org/10.1128/JVI.00789-08>.
  146. Sacramento CQ, de Melo GR, de Freitas CS, Rocha N, Hoelz LVB, Miranda M, Fintelman-Rodrigues N, Martorelli A, Ferreira AC, Barbosa-Lima G, Abrantes JL, Vieira YR, Bastos MM, de Mello Volotão E, Nunes EP, Tschoeke DA, Leomil L, Loliola EC, Trindade P, Rehen SK, Bozza FA, Bozza PT, Boechat N, Thompson FL, de Filippis AMB, Brüning K, Souza TML. 2017. The clinically approved antiviral drug sofosbuvir inhibits Zika virus replication. *Sci Rep* 7:40920. <https://doi.org/10.1038/srep40920>.
  147. Dhanwani R, Khan M, Bhaskar ASB, Singh R, Patro IK, Rao PVL, Parida MM. 2012. Characterization of Chikungunya virus infection in human neuroblastoma SH-SY5Y cells: role of apoptosis in neuronal cell death. *Virus Res* 163:563–572. <https://doi.org/10.1016/j.virusres.2011.12.009>.
  148. Huang H-I, Chang Y-Y, Lin J-Y, Kuo R-L, Liu H-P, Shih S-R, Wu C-C. 2016. Interactome analysis of the EV71 5' untranslated region in differentiated neuronal cells SH-SY5Y and regulatory role of FBP3 in

- viral replication. *Proteomics* 16:2351–2362. <https://doi.org/10.1002/pmic.201600098>.
149. Vesanen M, Salminen M, Wessman M, Lankinen H, Sistonen P, Vaheri A. 1994. Morphological differentiation of human SH-SY5Y neuroblastoma cells inhibits human immunodeficiency virus type 1 infection. *J Gen Virol* 75:201–206.
  150. Recio JA, Martinez de la Mata J, Martin-Nieto J, Aranda A. 2000. Retinoic acid stimulates HIV-1 transcription in human neuroblastoma SH-SY5Y cells. *FEBS Lett* 469:118–122. [https://doi.org/10.1016/S0014-5793\(00\)01249-7](https://doi.org/10.1016/S0014-5793(00)01249-7).
  151. Zhu X, Yao H, Peng F, Callen S, Buch S. 2009. PDGF-mediated protection of SH-SY5Y cells against Tat toxin involves regulation of extracellular glutamate and intracellular calcium. *Toxicol Appl Pharmacol* 240: 286–291. <https://doi.org/10.1016/j.taap.2009.06.020>.
  152. Peng F, Yao H, Akturk HK, Buch S. 2012. Platelet-derived growth factor CC-mediated neuroprotection against HIV Tat involves TRPC-mediated inactivation of GSK 3beta. *PLoS One* 7:e47572. <https://doi.org/10.1371/journal.pone.0047572>.
  153. Yaiw KC, Hyatt A, VanDriel R, Cramer SG, Eaton B, Wong MH, Wang LF, Ng ML, Bingham J, Shamala D, Wong KT. 2008. Viral morphogenesis and morphological changes in human neuronal cells following Tioman and Menangle virus infection. *Arch Virol* 153:865–875. <https://doi.org/10.1007/s00705-008-0059-0>.
  154. Préhaud C, Lay S, Dietzschold B, Lafon M. 2003. Glycoprotein of non-pathogenic rabies viruses is a key determinant of human cell apoptosis. *J Virol* 77:10537–10547. <https://doi.org/10.1128/JVI.77.19.10537-10547.2003>.
  155. Préhaud C, Wolff N, Terrien E, Lafage M, Megret F, Babault N, Cordier F, Tan GS, Maitrepierre E, Menager P, Choppy D, Hoos S, England P, Delepierre M, Schnell MJ, Buc H, Lafon M. 2010. Attenuation of rabies virulence: takeover by the cytoplasmic domain of its envelope protein. *Sci Signal* 3:ra5. <https://doi.org/10.1126/scisignal.2000510>.
  156. Takenouchi A, Saito K, Saito E, Saito T, Hishiki T, Matsunaga T, Isegawa N, Yoshida H, Ohnuma N, Shirasawa H. 2015. Oncolytic viral therapy for neuroblastoma cells with Sindbis virus AR339 strain. *Pediatr Surg Int* 31:1151–1159. <https://doi.org/10.1007/s00383-015-3784-y>.
  157. Zhang X, Zheng Z, Shu B, Mao P, Bai B, Hu Q, Cui Z, Wang H. 2016. Isolation and characterization of a Far-Eastern strain of tick-borne encephalitis virus in China. *Virus Res* 213:6–10. <https://doi.org/10.1016/j.virusres.2015.11.006>.
  158. Ninomiya K, Kanayama T, Fujieda N, Nakayama T, Komase K, Nagata K, Takeuchi K. 2009. Amino acid substitution at position 464 in the haemagglutinin-neuraminidase protein of a mumps virus Urabe strain enhanced the virus growth in neuroblastoma SH-SY5Y cells. *Vaccine* 27:6160–6165. <https://doi.org/10.1016/j.vaccine.2009.08.020>.
  159. Elankumaran S, Rockemann D, Samal SK. 2006. Newcastle disease virus exerts oncolysis by both intrinsic and extrinsic caspase-dependent pathways of cell death. *J Virol* 80:7522–7534. <https://doi.org/10.1128/JVI.00241-06>.
  160. Chen X, Quan R, Guo X, Gao L, Shi J, Feng W. 2014. Up-regulation of pro-inflammatory factors by HP-PRRSV infection in microglia: implications for HP-PRRSV neuropathogenesis. *Vet Microbiol* 170:48–57. <https://doi.org/10.1016/j.vetmic.2014.01.031>.
  161. Temonen M, Vapalahti O, Holthöfer H, Brummer-Korvenkontio M, Vaheri A, Lankinen H. 1993. Susceptibility of human cells to Puumala virus infection. *J Gen Virol* 74:515–518.
  162. Kim GN, Wu K, Hong JP, Awamleh Z, Kang CY. 2015. Creation of matrix protein gene variants of two serotypes of vesicular stomatitis virus as prime-boost vaccine vectors. *J Virol* 89:6338–6351. <https://doi.org/10.1128/JVI.00222-15>.
  163. Maldonado H, Ortiz-Riaño E, Krause B, Barriga A, Medina F, Pando ME, Alberti C, Kettlun AM, Collados L, García L, Cartier L, Valenzuela MA. 2008. Microtubule proteins and their post-translational forms in the cerebrospinal fluid of patients with paraparesis associated with HTLV-I infection and in SH-SY5Y cells: an in vitro model of HTLV-I-induced disease. *Biol Res* 41:239–259. <https://doi.org/10.4067/S0716-97602008000300001>.